An Examination of Lake Erie's "Western Basin Occupying" Yellow and White Perch Populations from a Graph Theory Perspective

Caitlyn Feldpausch
Carthage College
cfeldpausch@carthage.edu, 308cait2019@gmail.com

July 21, 2025

Abstract

Although Lake Erie is one of the Great Lakes life-rich ecosystems, its traits are continually tracked and analyzed to ensure future freshwater health. A key lies in understanding the development of native and invasive fish populations. With that knowledge, we may compare these populations to consecutively smaller or larger organism dynamics. Gathering research that analyzes freshwater systems is how national organizations tackle freshwater issues. A typical avenue of investigation utilizes data collection and statistical analysis to determine species relationships. Instead, we apply an avenue of approach via graph theory. We gather data on Lake Erie's western basin, allowing examination of the native white and yellow perch populations' analogous or cross-pernicious trends, finding they are due to diet and ecosystem health agents.

1 Introduction

Three data sets were found from the United States Geological Survey (USGS) for this freshwater analysis. The United States Geological Survey is a credible government organization that collects data on geoscience related issues from agriculture to infrastructure. This involves in situ field and satellite collected data which we will touch on further as a method of future analysis.

The Lake Erie Fish Community data set is our first one used. It will be used to understand diet and competition characteristics of the perch populations. Data taken from the USGS records many different fish species, the type of prey they consumed, and the amount of that prey consumed in grams. It also includes other recordings such as latitude and longitude of sample collection sites, but we are less interested in this data. The data is reported on a yearly basis to give estimates of densities of key forage and predator species in the western basin of Lake Erie, and to assess seasonal and spatial distributions of fish with water quality information along with year class strength Schmitt. [1].

Figures 25-28 report two dreissenid species dry weights, those of the zebra mussel and quagga mussel, for both the shell and flesh parts of the organism that were present in fish stomachs [2]. There is much research on dreissenid mussels on the Great Lakes. This data seeks to grow knowledge on mussel abundance variation mechanisms and answer "how much mussel biomass is consumed by fish predation" [2]. This is hard to answer due to the mussel's weight including shell parts. The data is used to better estimate flesh dry weights of the mussels in fish diets. Analysis of the dry weights has simulated fish stomach contents "ranging from small (individual mussels) to large (aggregates of mussels)" [2]. Collections occurred in 2014 at the Sandusky, Ohio USGS biological station at Lake Erie. We will use this data set to analyze if invasive quagga mussels or native zebra mussels were preferred, and by either shell or flesh parts.

Phytoplankton Community Composition in Western Lake Erie is our final data set. We will use it to examine overall ecosystem health and provide future research prospects. It contains a tabular file of phytoplankton abundance and community composition analysis in samples collected from eight sites in the west basin of Lake Erie; four sites at Grand Traverse Bay, Lake Michigan; and five sites at Saginaw Bay, Lake Huron [3]. We can note sample collection occurred in summer and early fall. The dataset includes phytoplankton taxa (genus and species), division, tally (number of cells counted for each taxa present), density (cells per liter), and total biovolume (cubic micrometers per liter) for each specimen [3]. The data can assess community composition of phytoplankton, identify kinds of cyanobacteria, and also determine abundance and biovolume of toxic cyanobacteria. Data was originally collected to assess phytoplankton abundance and cyanobacteria community composition from samples.

While examining and analyzing the above data sets, we not only tackle a new method of analysis for freshwater research, but also ensure multiple viewpoints are made while addressing similar questions. When studying freshwater science, we must properly apply the scientific method by using lots of data, having lots of trial and error, and making result reinforced conclusions.

2 Definitions and Development

Definition 1. G is **bipartite** if $V(G) = V_1 \cup V_2$ and $V_1 \cap V_2 = \emptyset : E(G) \subseteq < u_1, u_2 > | u_1 \in V_1, u_2 \in V_2$ [4].

Definition 2. $H \subseteq G$ is a **component** of G if H is connected and not contained in a connected subgraph of G with more vertices or edges. The number of components of G is $\omega(G)$ [4].

Definition 3. For a graph G let $E^* \subset E(G)$. If $\omega(G - E^*) > \omega(G)$ then E^* is called an **edge cut** [4].

Definition 4. Two sets are **disjoint** if they have no two elements in common such that $A \cap B = \emptyset$ [5].

Definition 5. The number of edges incident on a vertex v is the **degree** of v, denoted as $\delta(v)$ [4].

First we note that although most graphs below follow Definition 1, and are indeed bipartite, some graphs contain self loops which break Definition 1. Those graphs are thus not bipartite. Loops, or edges joining a vertex with itself, get counted twice [4]. We will start by analyzing the data as disaggregated or in broken down graphs. Then we will move on to the aggregated data's graphs which include the information as a whole.

Referring to the Lake Erie data set used for our first graphs, we should point out a vital assumption made. Since 2014 and/or 2015 and/or 2016 appeared in all data sets, to compare and contrast between them, all other yearly data was removed. We can see in the first figures that the data is filtered to white and yellow perch species. These figures then include their subsequent prey weights eaten. There are two types of nodes, either yellow or white perch species, and then the prey they ate. Edges are weighted by the sum of consumed prey weight in grams per prey type. For example, if scientists recorded a sample of round goby prey weight in yellow perch on multiple occasions, the round goby edge weight is then a sum of those samples. In this graph set we will be answering the following questions. When removing edges of weight below or equal to a threshold value, what percent of the total weight is lost? Which prey is most popular by identifying the greatest value edge weight? If edges of minimal 'prey weight g' are cut out when below a threshold weight, do disjoint sets appear? How does this change year-to-year? How does this change between yellow and white perch? When removing edges of weight below a threshold value for both species simultaneously, and in a given year, what percent of the total weight is lost?

Figure 24 uses the same data as the first graph set, but this time our nodes change. Nodes are the type of prey eaten and the corresponding year(s) that they were eaten. Edge weights are the same designation of the sum of prey weight in grams per prey type. Here we ask if Figure 24 supports our first graph set's prey type popularity analysis or highlights another point?

Our third graph set has four graphs, broken down by flesh or shell dry weights and by mussel type. Figures 25-28 had their year range cut to 2014-2016 for the purpose of matching results and data collection time frames, to avoid analysis error and outlying data. Nodes are the type of dreissenid and either flesh or shell dry weight. Edge weights are the dry weight value in grams. For these graphs, we seek to know if a higher total edge weight for either quagga or zebra mussels can help explain earlier conclusions in the first graph set.

Figure 30 displays the biovolume of phytoplankton that are present in two types of samples. These biovolumes are our edge weights in cubic micrometers per liter. Nodes are either sample type (sediment or water) or phytoplankton division. "Division" refers to a type of taxa classification. By rank, "division" falls under "kingdom". For these graphs we ponder where most of the biomass exists by calculating the phytoplankton biovolume sum for each sample type and seeing which is higher? Based on this answer, we will determine if excess phytoplankton in a sample type is more or less detrimental than if there were an excess in the other.

To analyze competition and diet trends of the Lake Erie ecosystem, we make edge cuts to our graphs and understand how a decrease in prey might affect these trends in real life or in the pre-selected year range from our data. We can see what percentage of total prey weight is lost by assigning a threshold edge weight and making edge cuts, as Definition 3 stipulates, which are equal to or below that threshold value. To understand what an edge cut entails, we must know what components are by Definition 2. When determining a threshold weight, we examine the range and frequency of values.

Looking at the raw data of individual prey consumption and Figure 1 we can tell there is an increase in prey weight when the count (the height of columns appearing before 1 gram on the horizontal axis) is less than 1 gram, and a drop in prey weight when the count is greater than 1 gram. When you sum the prey weights greater than one for both species you get 31.5 grams. When you sum the prey weights less than one for both species you get 55.4 grams. Thus, a large amount of consumed prey is eaten in small portions. This tells us that prey species below the one gram cutoff are likely 'incidental' prey that are consumed based on availability. Those above the cutoff are more 'main' prey. Initial examination and graphical analysis have set 1 gram as a decent threshold. Let us graphically analyze further to arrive at more accurate threshold weights.

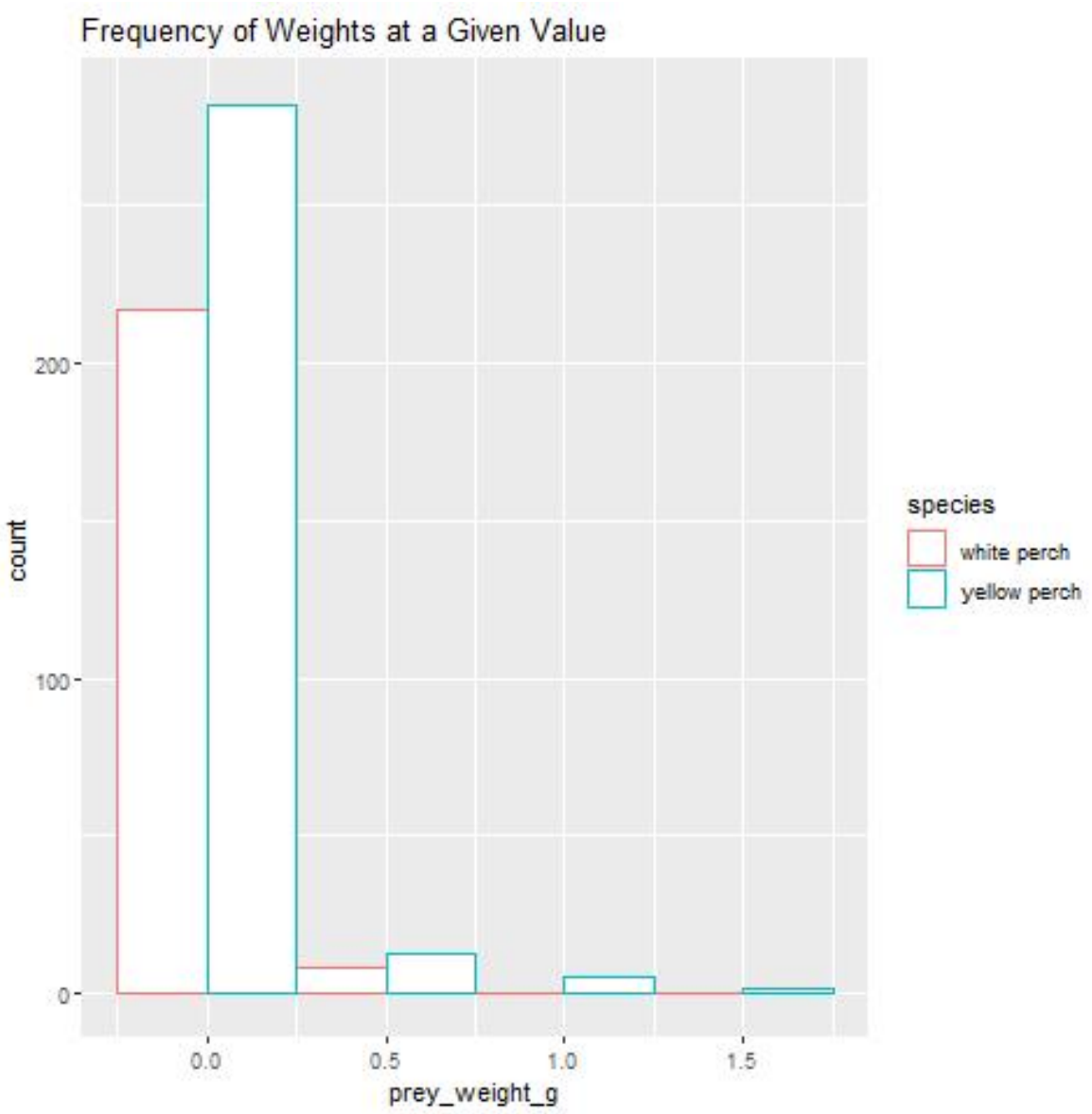

Figure 1: A histogram of the number of times prey weights are recorded between 2014 and 2016 and at a given value for white or yellow perch species

We can see in Figure 2 that threshold weights have a relatively steady slope by increasing percentages of weight removed. We decide to choose a close threshold value to where this nice distribution of percent values and steady slope changes. We do this since the steady slope denotes a gap in the weight distributions. In red, 2014 appears to leave this smoother inclination at about 1.5 grams. In blue, 2015 seems to leave this smoother inclination at about 0.7 grams. Lastly, 2016, in green, leaves this smoother inclination at about 0.9 grams. Therefore, we have three threshold weights, one for each year, based on where slopes departed from a clean and similarly logarithmic trend.

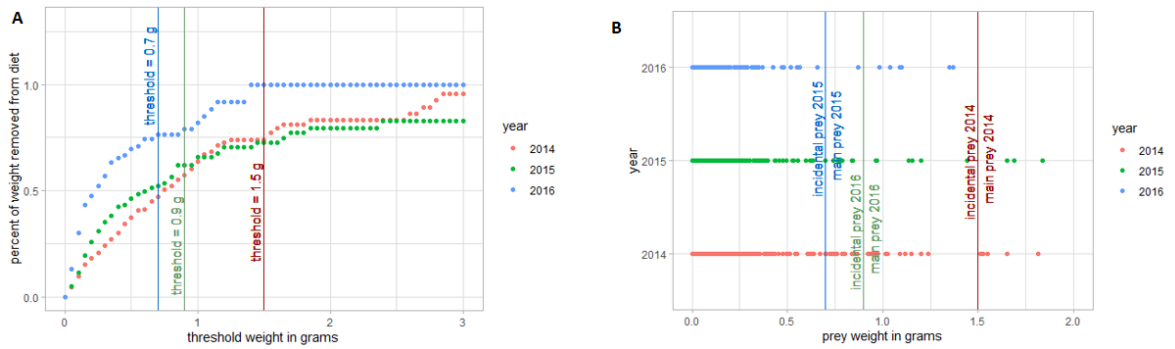

Figure 2: With three different thresholds, panel a (left) displays the removed percent of prey weight in grams for both perch species in 2014, 2015, and 2016. Panel b depicts grams of prey weights by year with cutoff thresholds marked for the 'incidental' and 'main' prey together

Assigning the above threshold weights and making edge cuts when the weight is below those values leads to the following Figures 3-14 and our Figure 15 percentages in our Results section. Percentages represent the total prey weight recorded per species and year. Percentages also come from edge weights, or sums of all recorded prey weights for a given prey type. On a graphical note, the edge cuts result in Definition 4 disjoint sets for Figures 3, 5, 7, 9, 11, and 13. These revised graphs, Figures 4, 6, 8, 10, 12, and 14, are also in our Results section.

3 Results

As stated in our Development section, nodes indicate perch and prey species, edges indicate predation, and edge weights indicate the total biomass of that prey type eaten by the perch species in a given year.

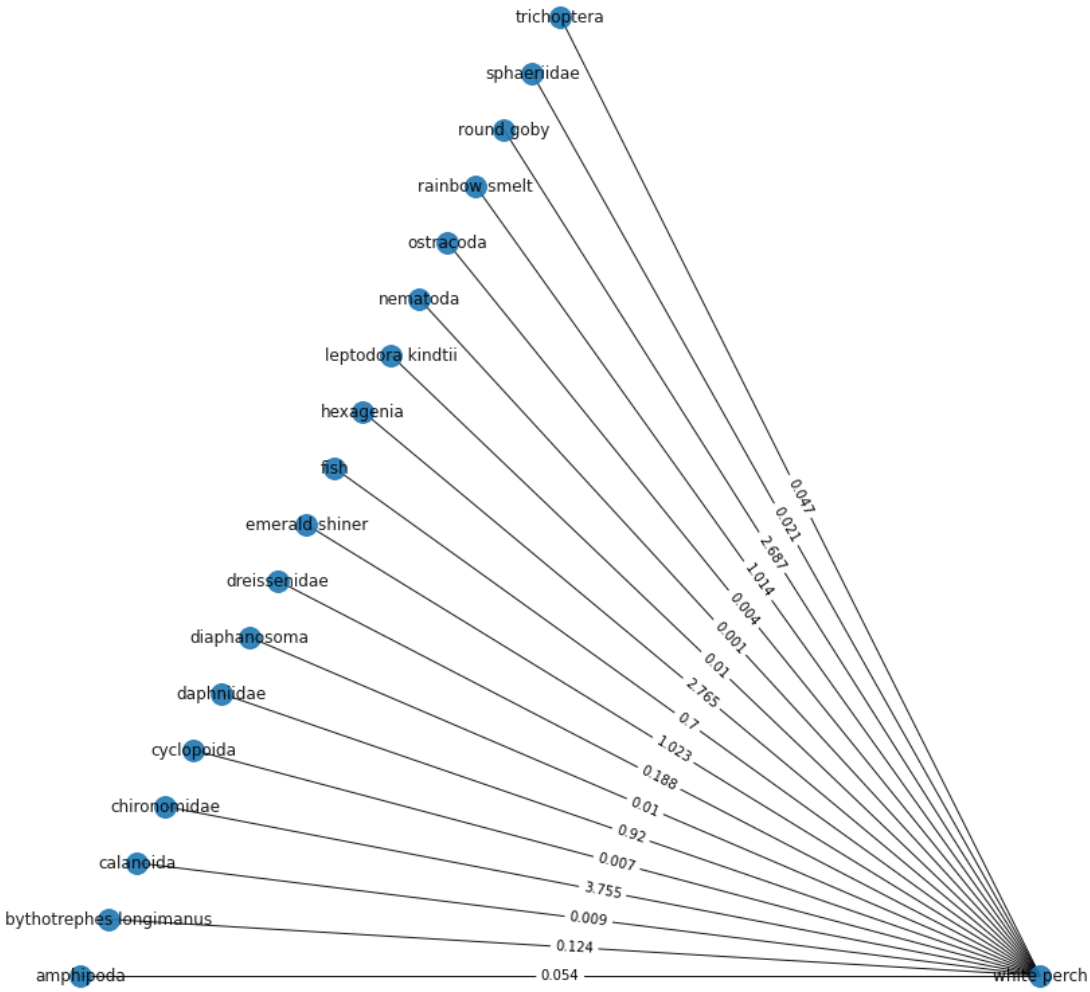

Figure 3: White perch consumed prey type and amount in grams for 2014

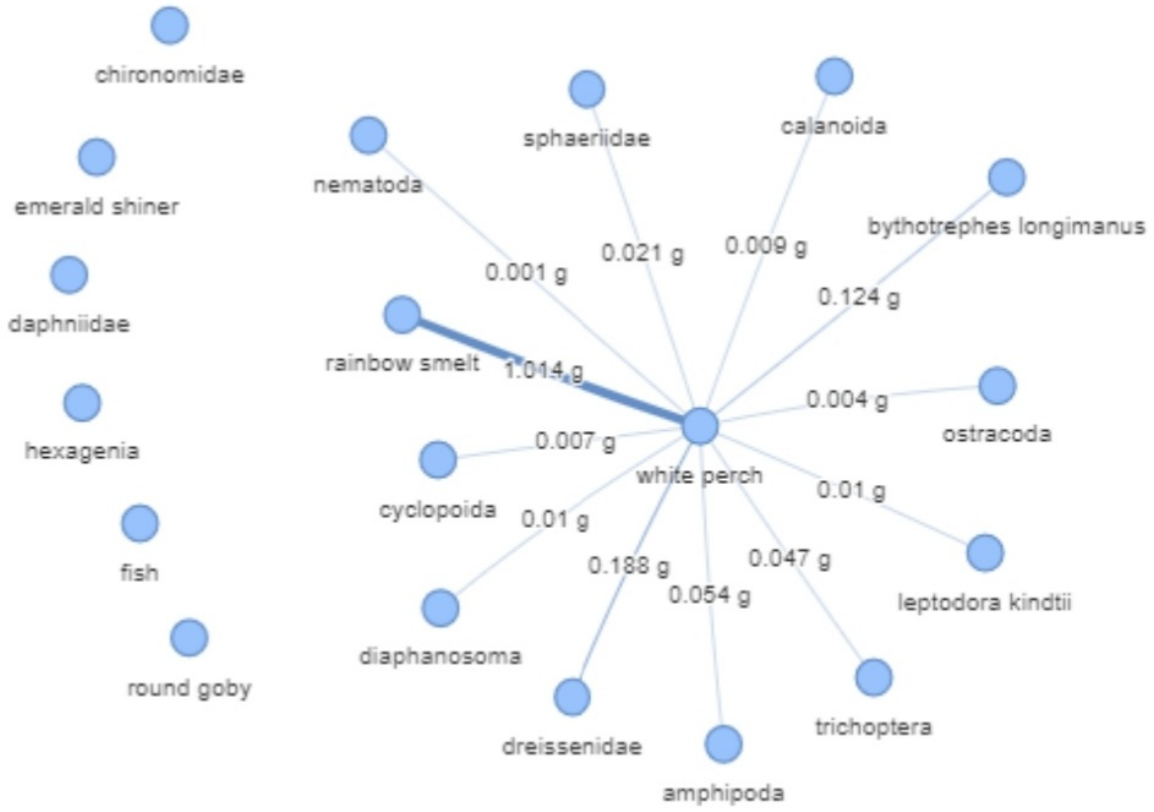

Figure 4: A disjoint set resulting from edge cuts made to Figure 3 when prey weight was below 1.5 grams. Disconnected nodes account for 11.2% of the white perch diet in 2014

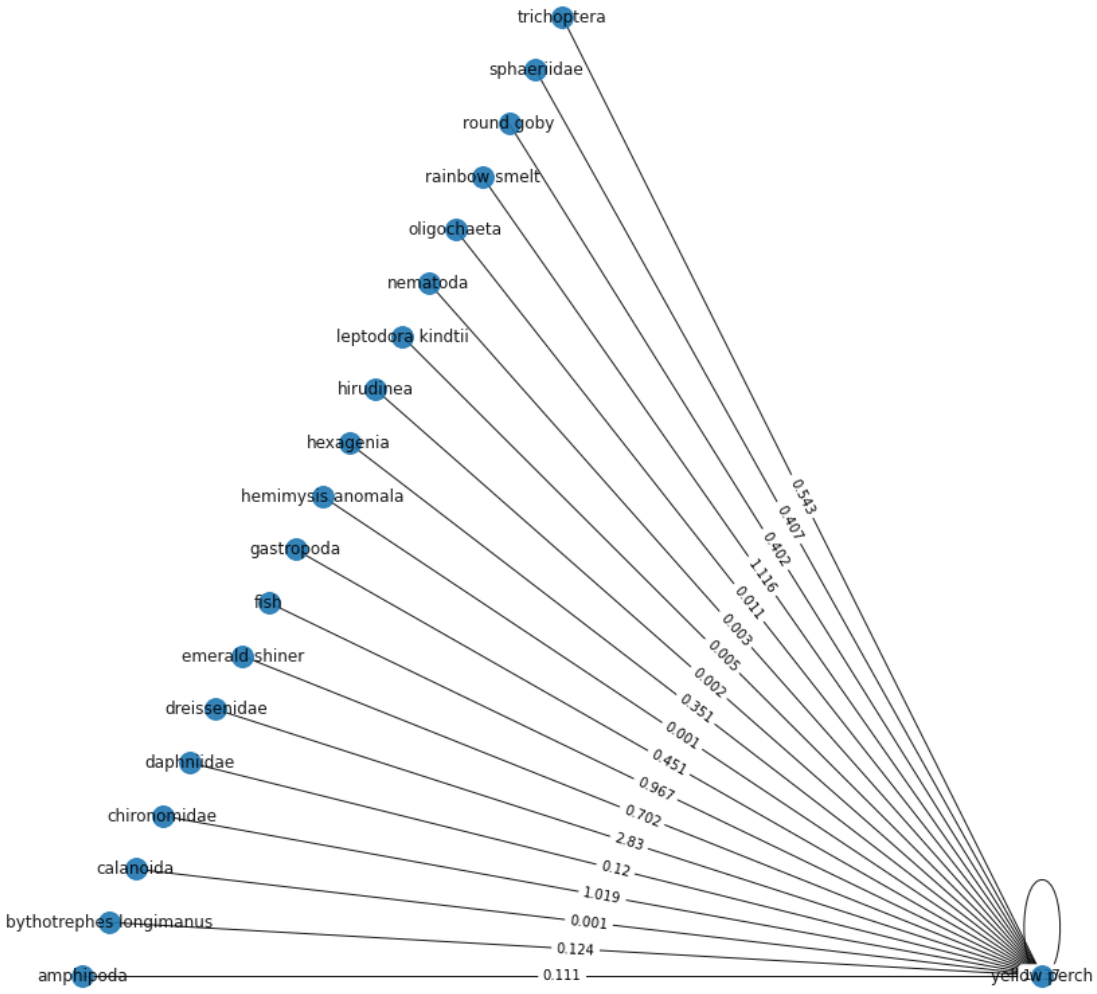

Figure 5: Yellow perch consumed prey type and amount in grams for 2014

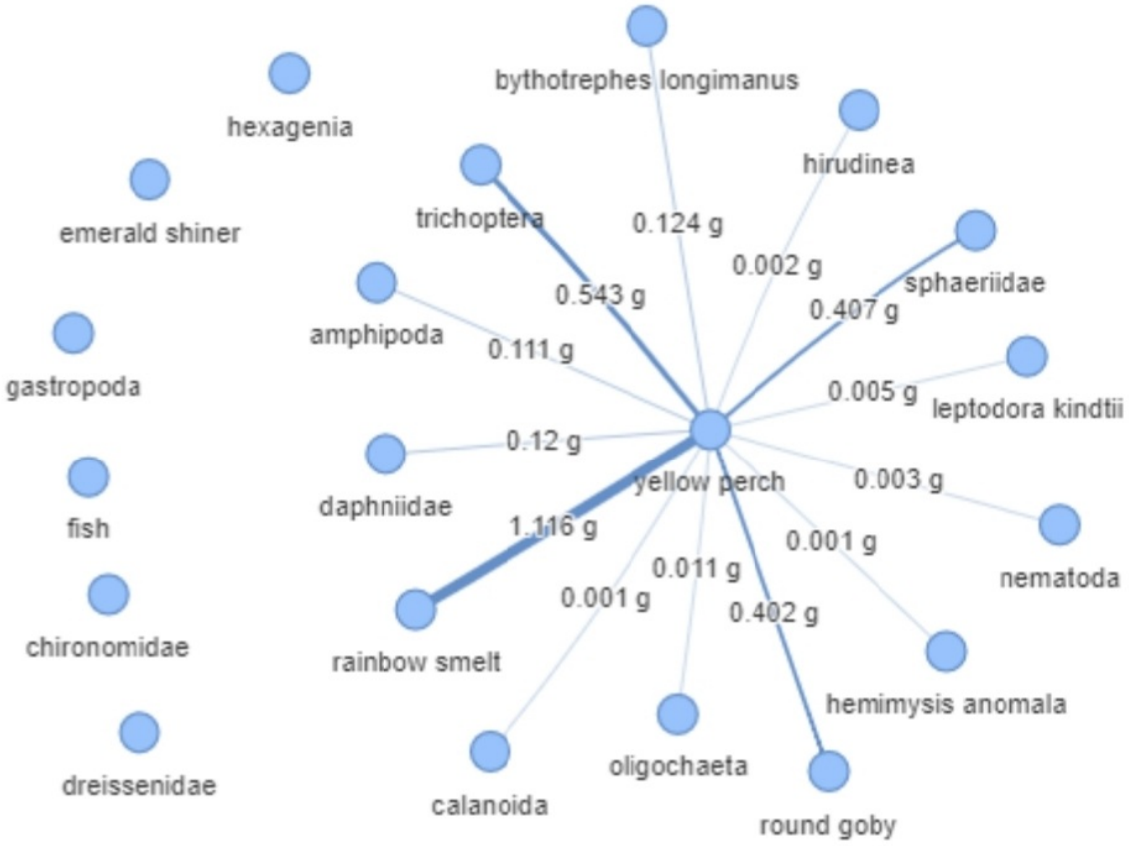

Figure 6: A disjoint set resulting from edge cuts made to Figure 5 when the threshold weight was below 1.5 grams. Disconnected nodes account for 31.1% of the yellow perch diet in 2014

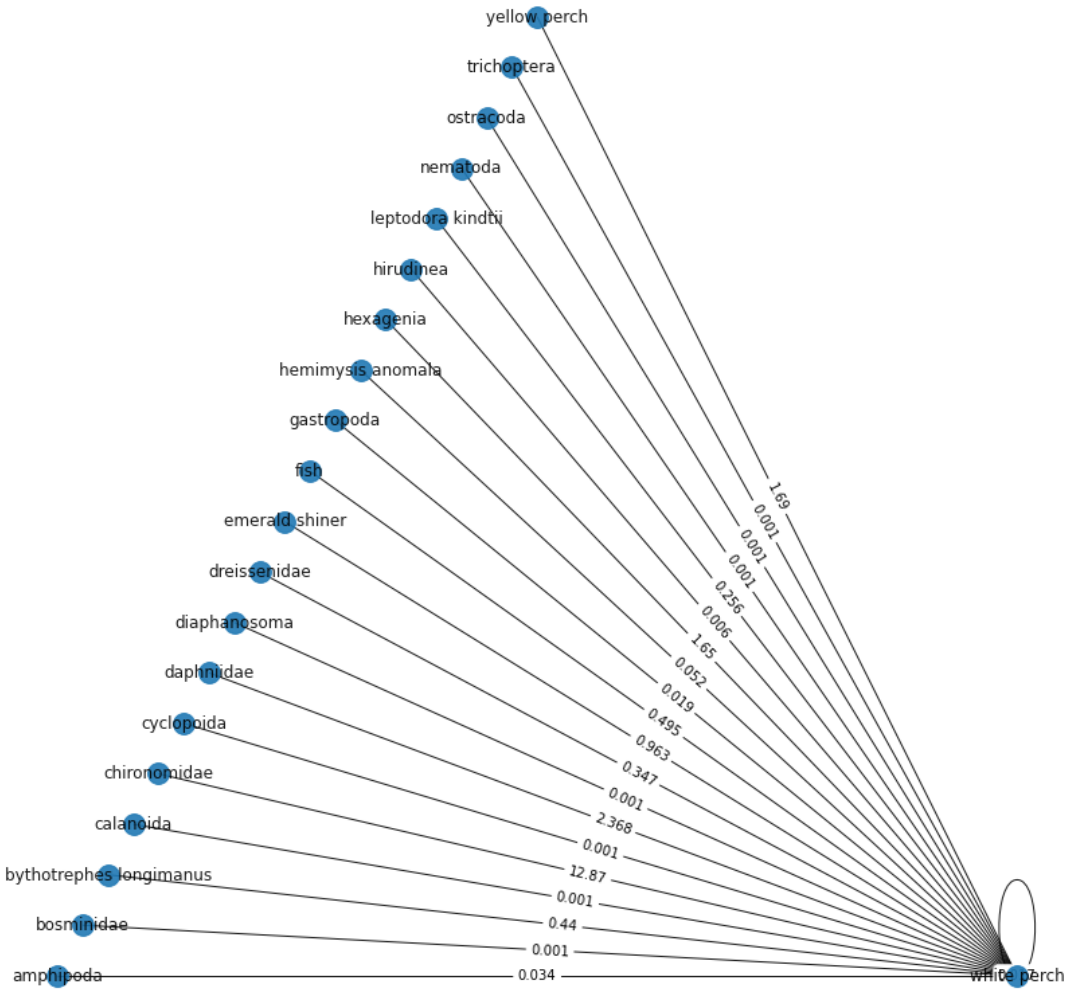

Figure 7: White perch consumed prey type and amount in grams for 2015

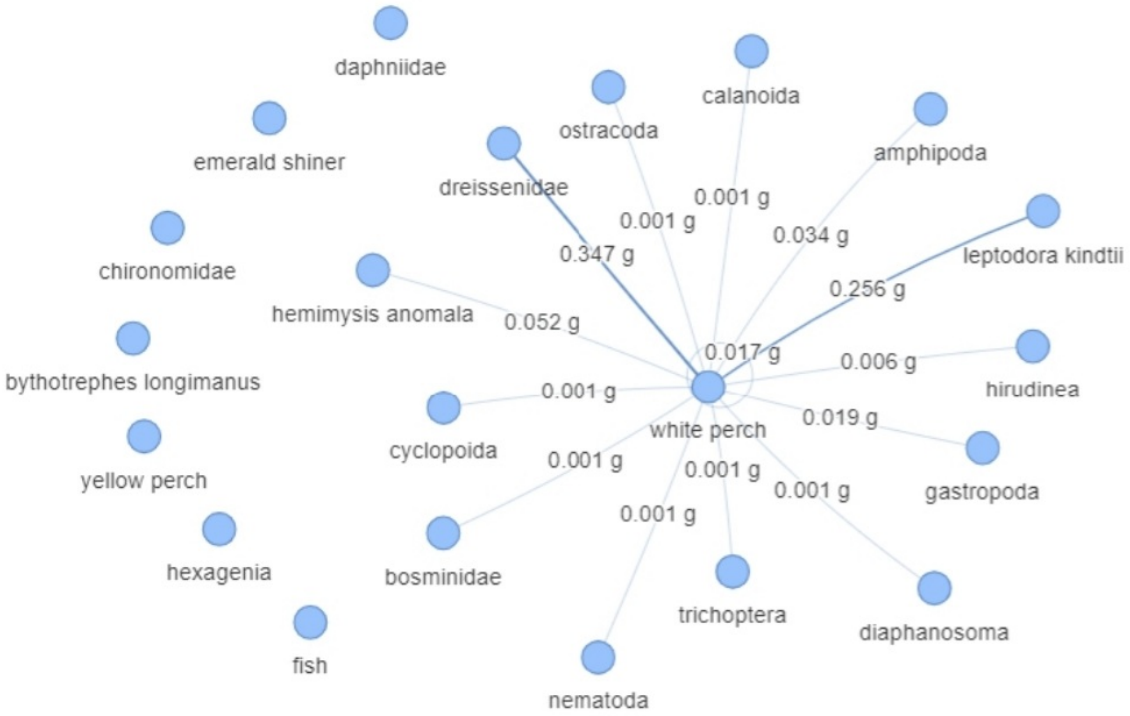

Figure 8: AA disjoint set resulting from edge cuts made to Figure 7 when the threshold weight was below 0.7 grams. Disconnected nodes account for 3.4% of the white perch diet in 2015

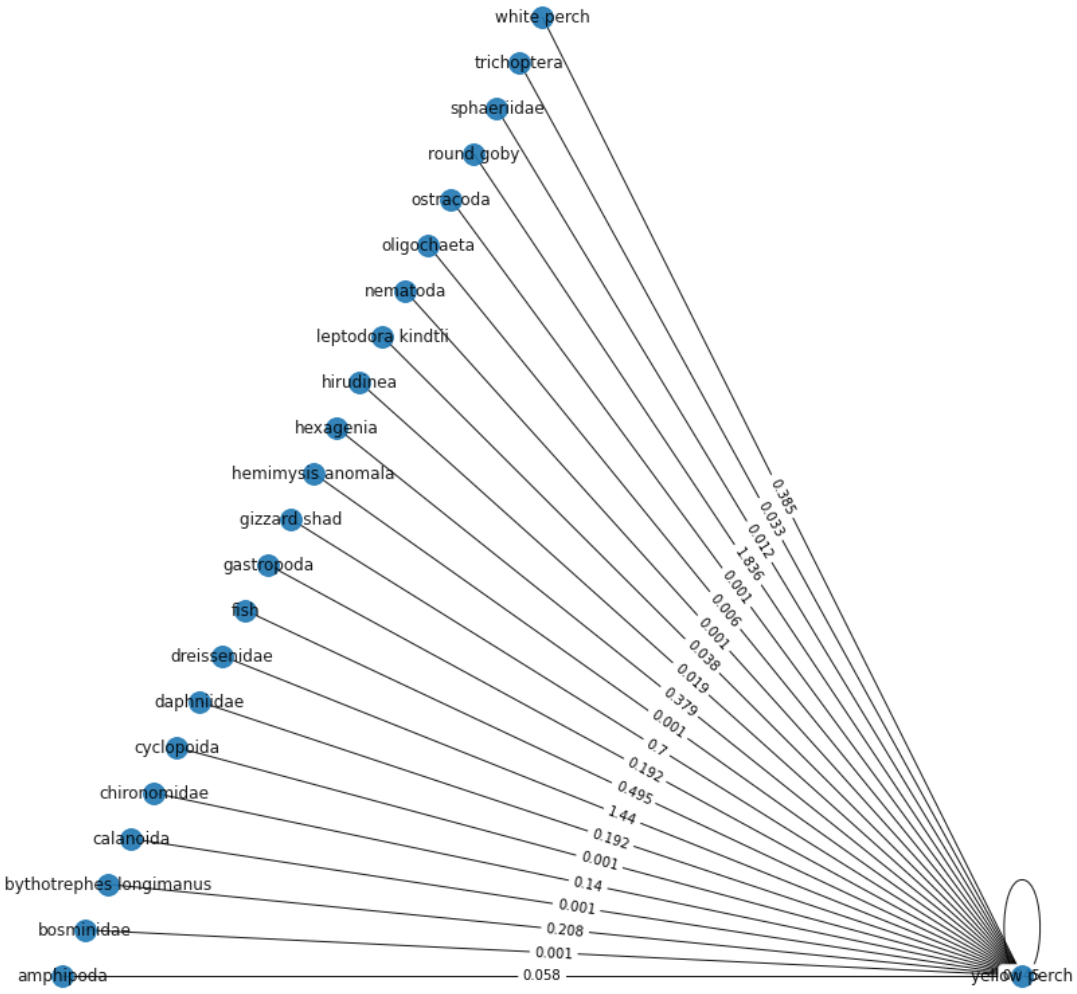

Figure 9: Yellow perch consumed prey type and amount in grams for 2015

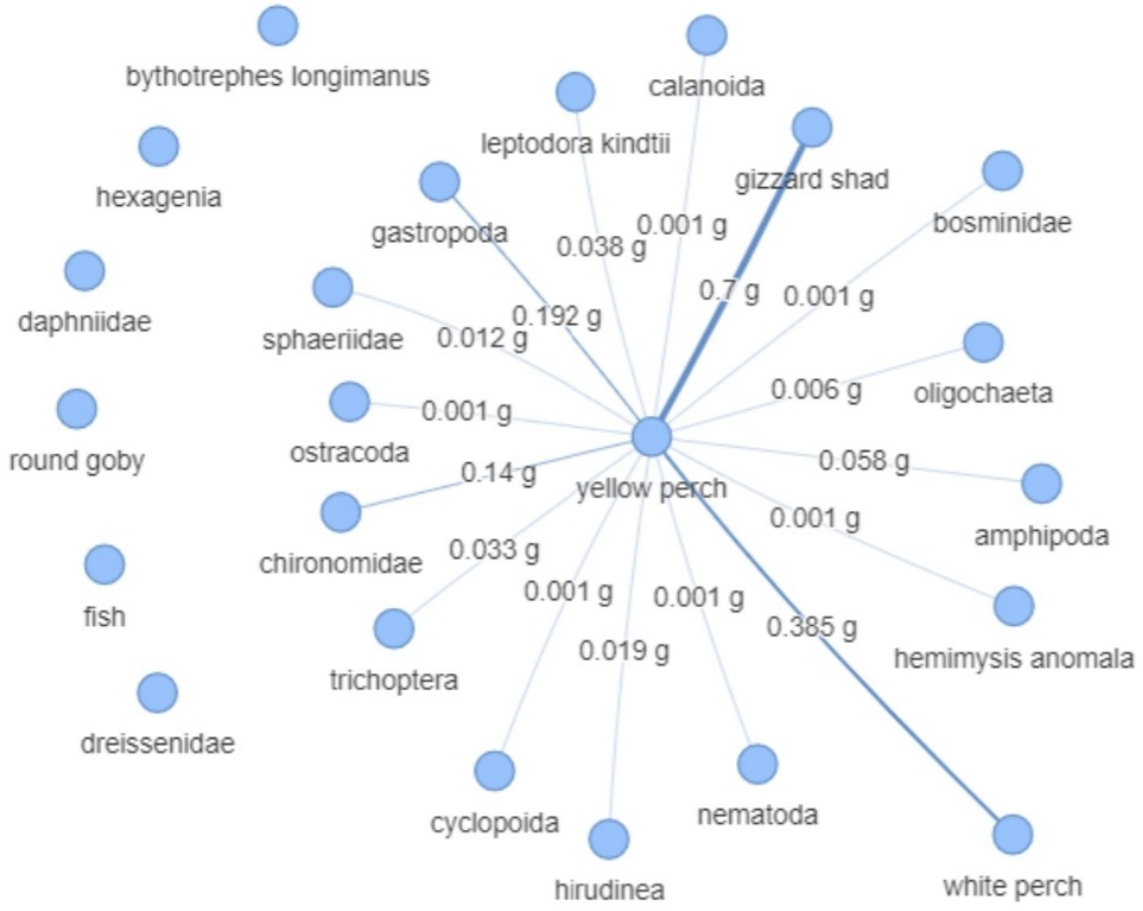

Figure 10: A disjoint set resulting from edge cuts made to Figure 9 when the threshold weight was below 0.7 grams. Disconnected nodes account for 25.8% of the yellow perch diet in 2015

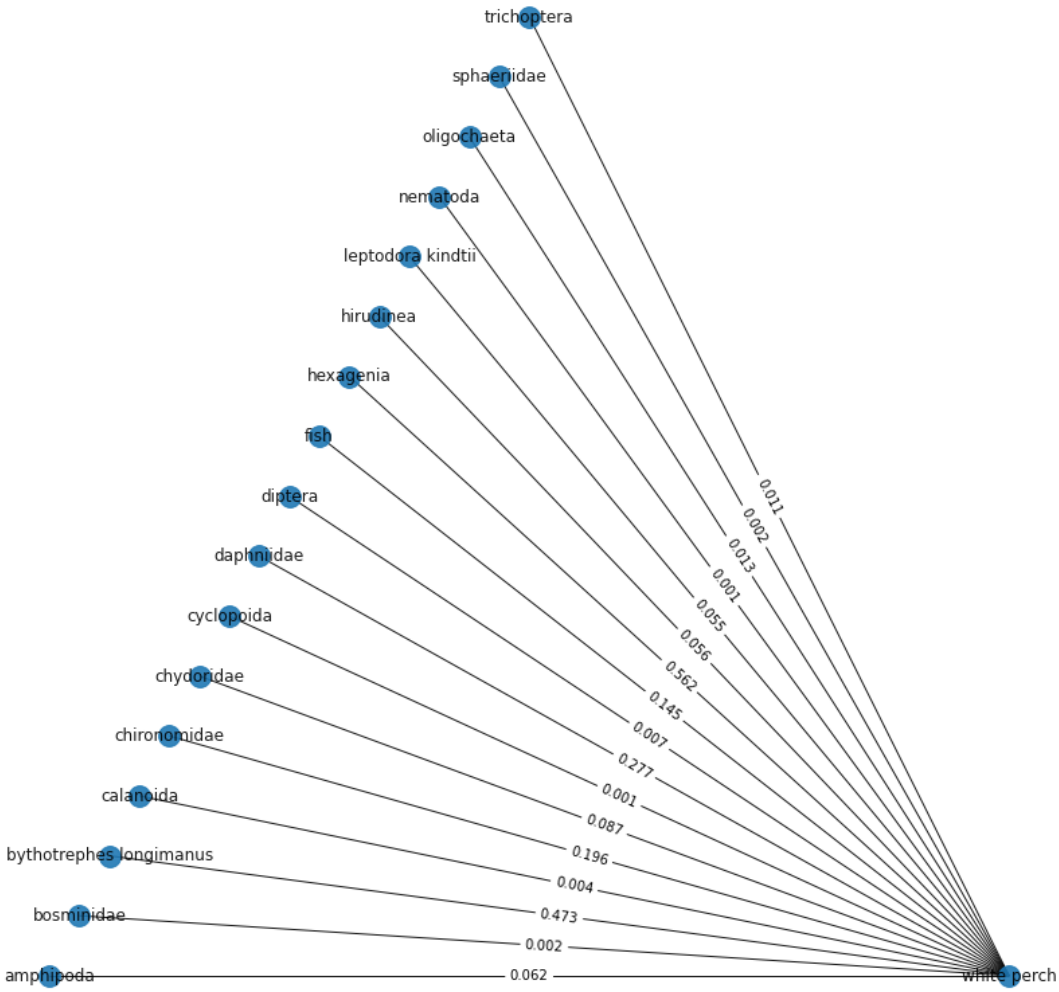

Figure 11: White perch consumed prey type and amount in grams for 2016

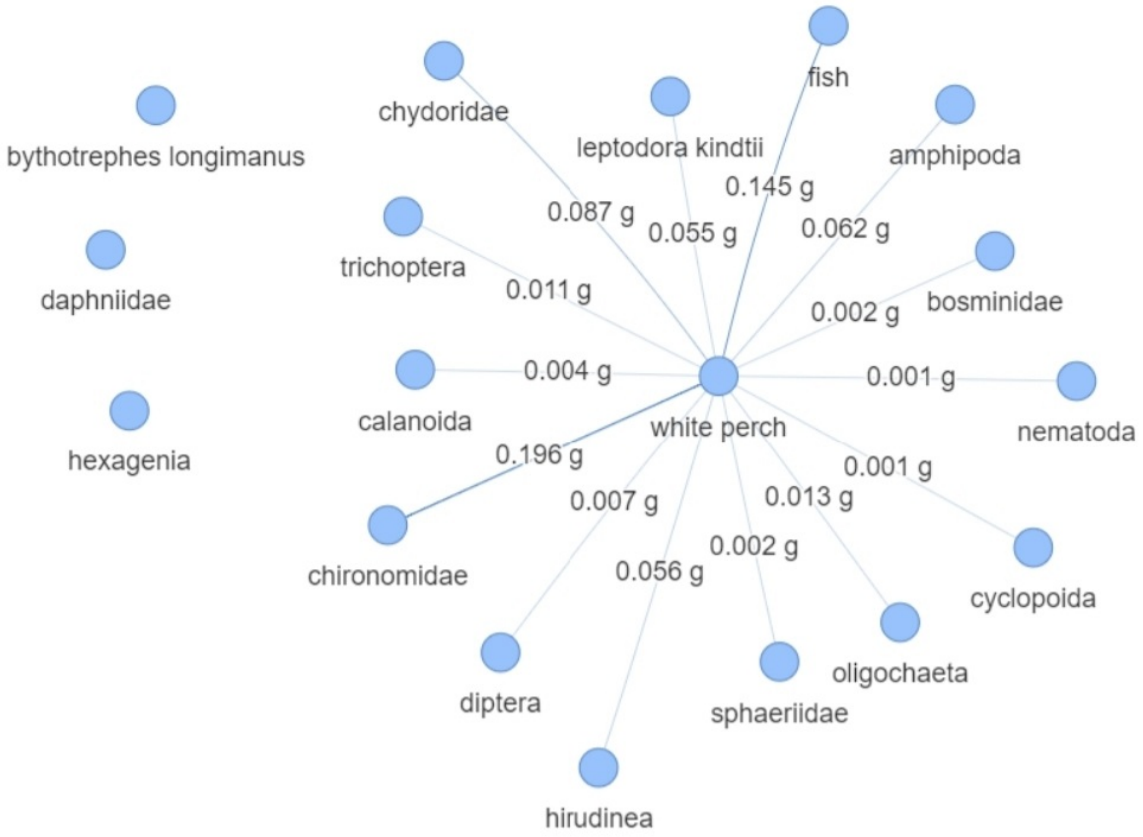

Figure 12: A disjoint set resulting from edge cuts made to Figure 11 when the threshold weight was below 0.9 grams. Disconnected nodes account for 32.8% of the white perch diet in 2016

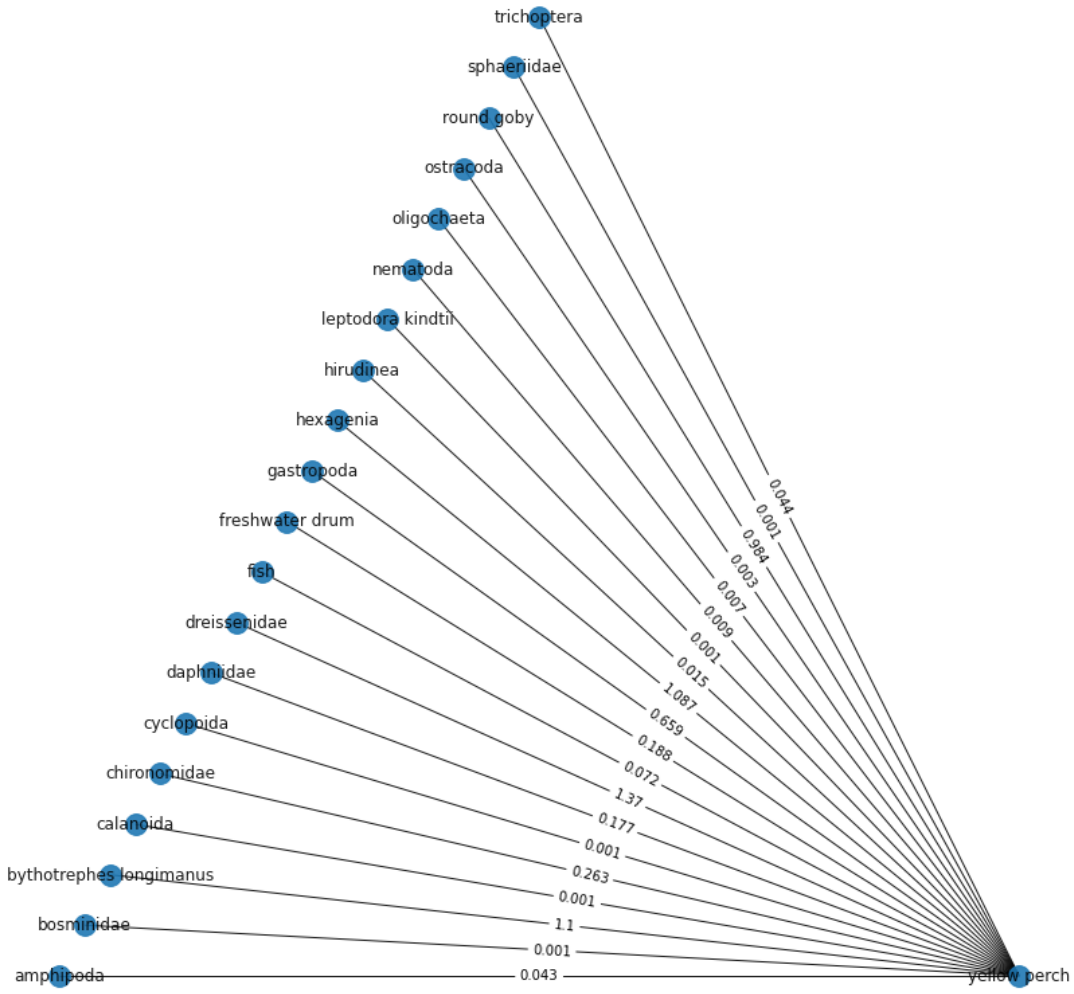

Figure 13: Yellow perch consumed prey type and amount in grams for 2016

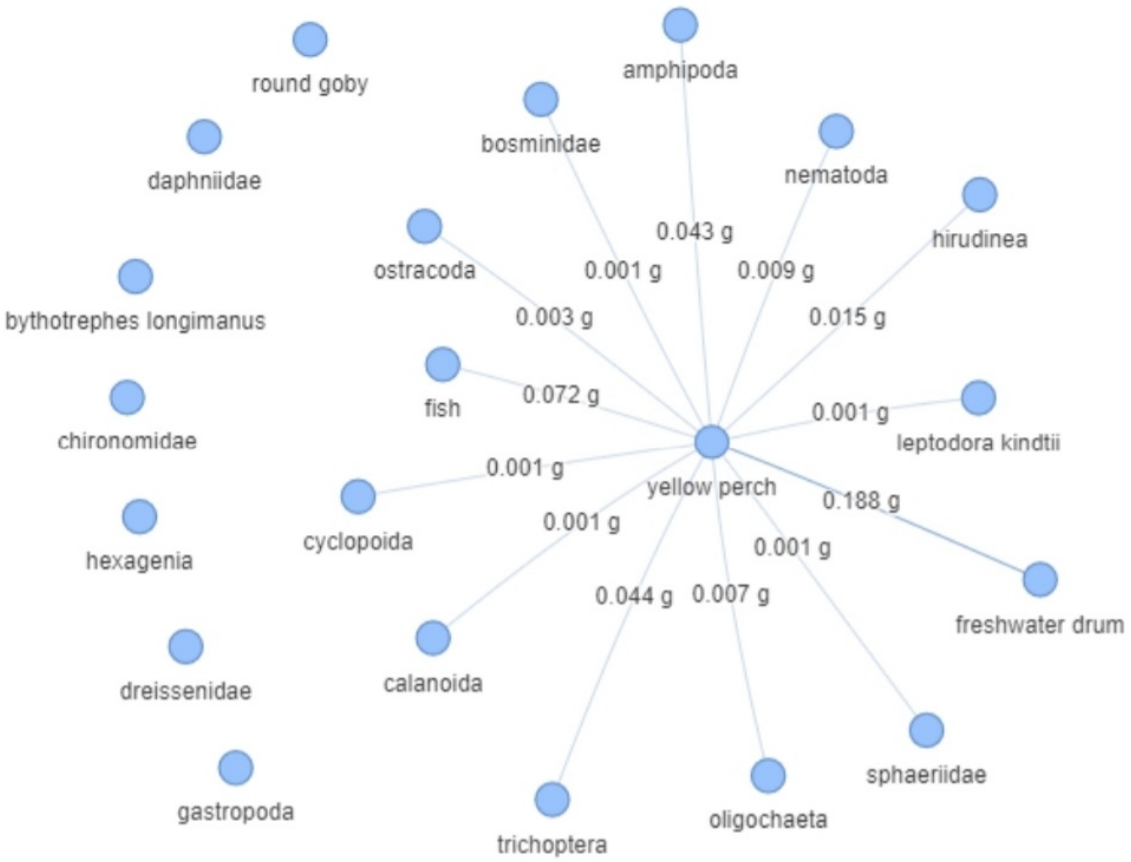

Figure 14: A disjoint set resulting from edge cuts made to Figure 13 when the threshold weight was below 0.9 grams. Disconnected nodes account for 6.4% of the yellow perch diet in 2016

Threshold Weight (g)	Year	White Perch % of Total Prey Lost	Yellow Perch % of Total Prey Lost
1.5	2014	11.2%	31.1%
0.7	2015	3.4%	25.8%
0.9	2016	32.8%	6.4%

Figure 15: Percentage of prey weight in grams taken out after making edge cuts to Figures 3, 5, 7, 9, 11, and 13 when the prey weight was at or below our threshold values

Through these threshold parameterized graphs, we calculate the percentage of prey weight lost in Figure 15. Then we discern when each perch species is most affected by the removed diet. Yellow perch are most affected in 2014, at 31.1%. White perch are most affected in 2016, at 32.8%. Even though we only took out consumed weights below 1.5 grams, 0.7 grams, and 0.9 grams, this accounts for a lot of the diet lost, but still less than 50%. By making the edge cuts, we cause the species to rely on the prey type they consume the most grams of, the 'main' prey. If this occurs in reality, we can also assume this creates extra competition between the two species due to the large percentage loss.

Year	White Perch	Yellow Perch
2014	Chironomidae	Dreissenidae
2015	Chironomidae	Round Goby
2016	Hexagenia	Dreissenidae

Figure 16: Most popular prey by perch species and year

Applying straightforward examination of Figures 3, 7, and 13, we complete Figure 16 detailing which prey was most popular by perch species and year. It is interesting that chironomidae is the most popular prey for white perch in 2014 and 2015. Due to continued popularity we assume this prey was abundant and accessible during those years. Dreissenidae is most popular in 2014 and 2016 for yellow perch. Maybe there is a correlation between this Dreissenidae popularity and our phytoplankton or mussel data and corresponding graph later on, especially since zebra mussels are in the dreissenidae family [6].

Now we will analyze the aggregated data of both species simultaneously in Figures 17, 19, and 21. Again utilizing edge cuts and the same threshold weights as before, we analyze the compiled graphs and arrive at our Figure 23 percentages. Again, edge cuts result in disjoint sets by Definition 4 as Figures 18, 20, and 22 pictured below.

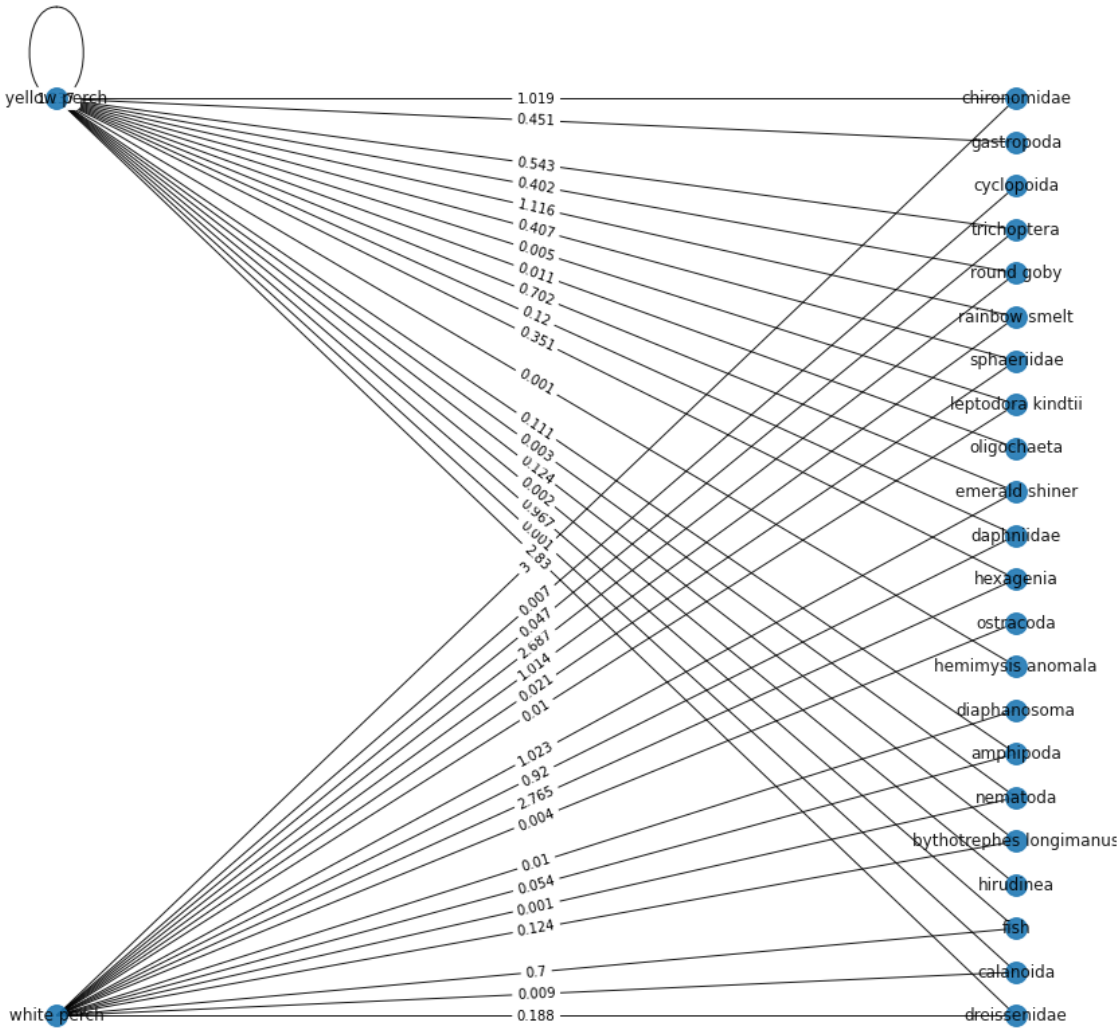

Figure 17: Both perch species consumed prey type and amount in grams for 2014

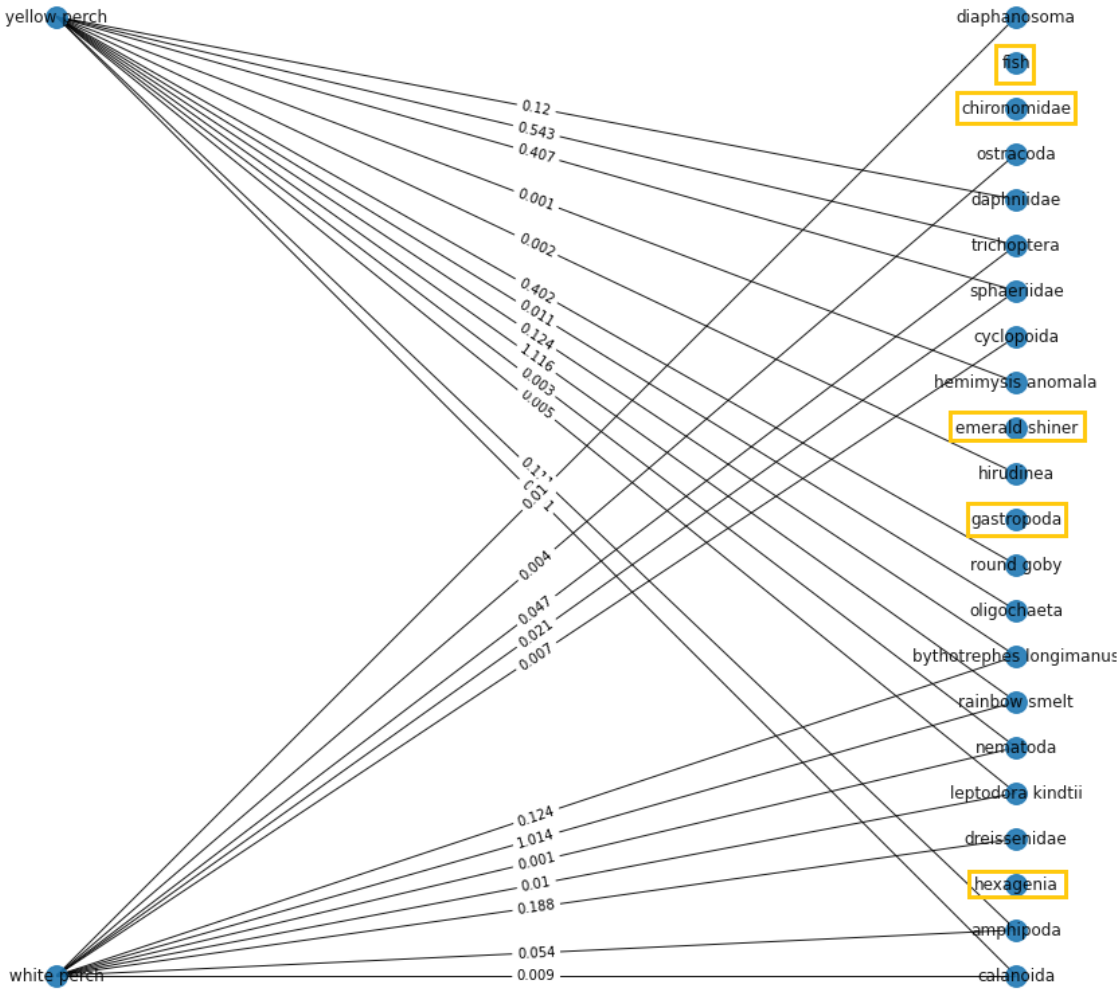

Figure 18: A disjoint set resulting from edge cuts made to Figure 17 when the prey weight was below 1.5 grams and consumed by both perch species in 2014. Prey no longer a member of the bipartite graph are boxed in yellow

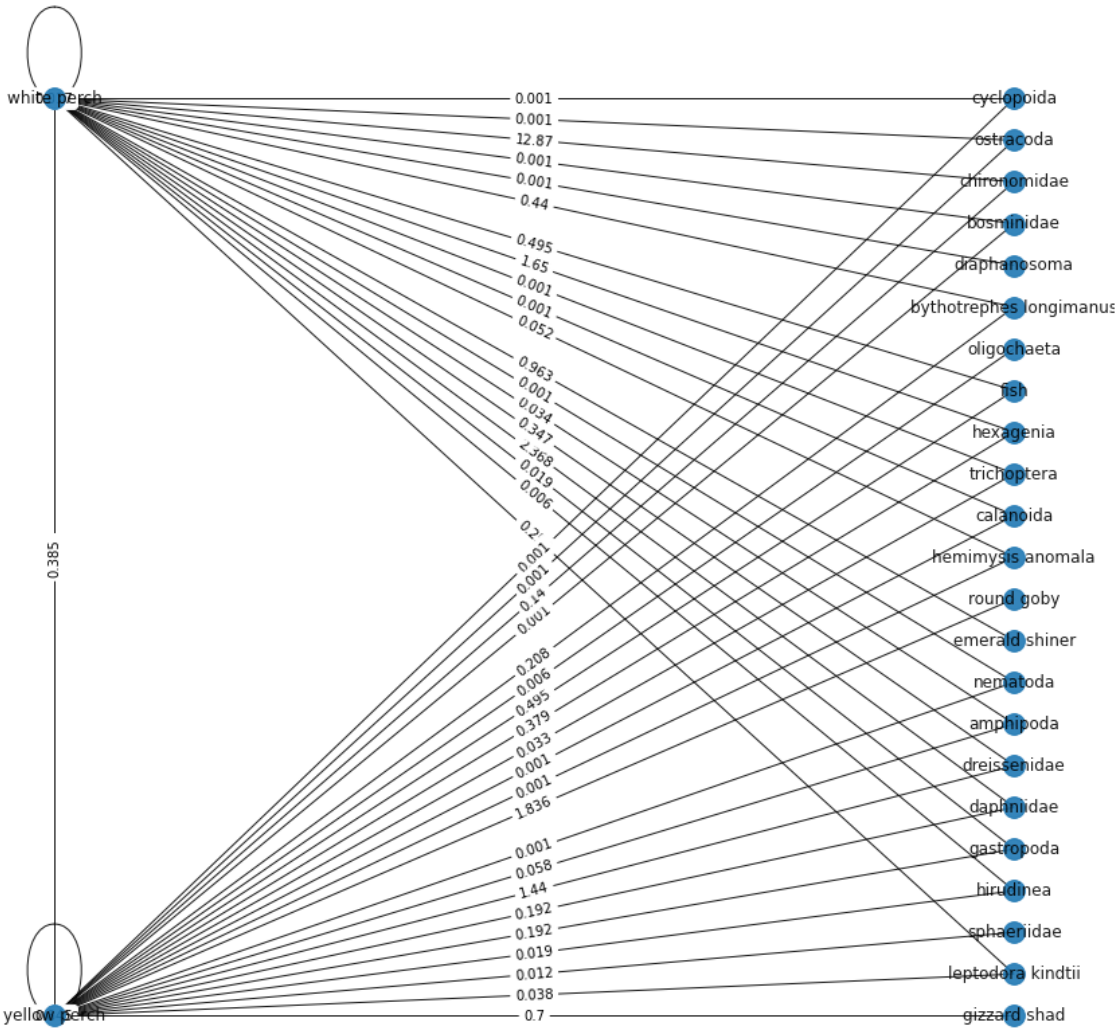

Figure 19: Both perch species consumed prey type and amount in grams for 2015

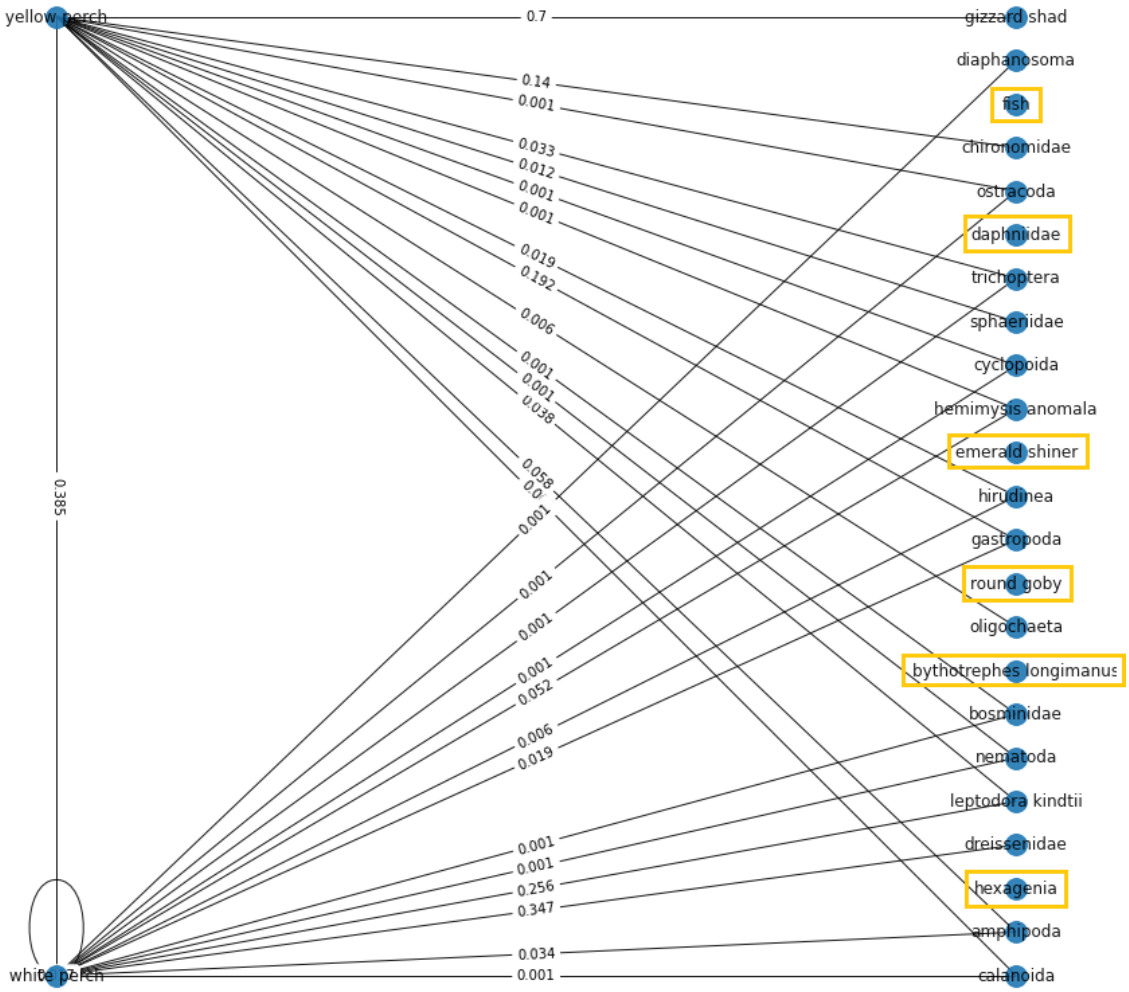

Figure 20: A disjoint set resulting from edge cuts made to Figure 19 when the prey weight was below 0.7 grams and consumed by both perch species in 2015. Prey no longer a member of the bipartite graph are boxed in yellow

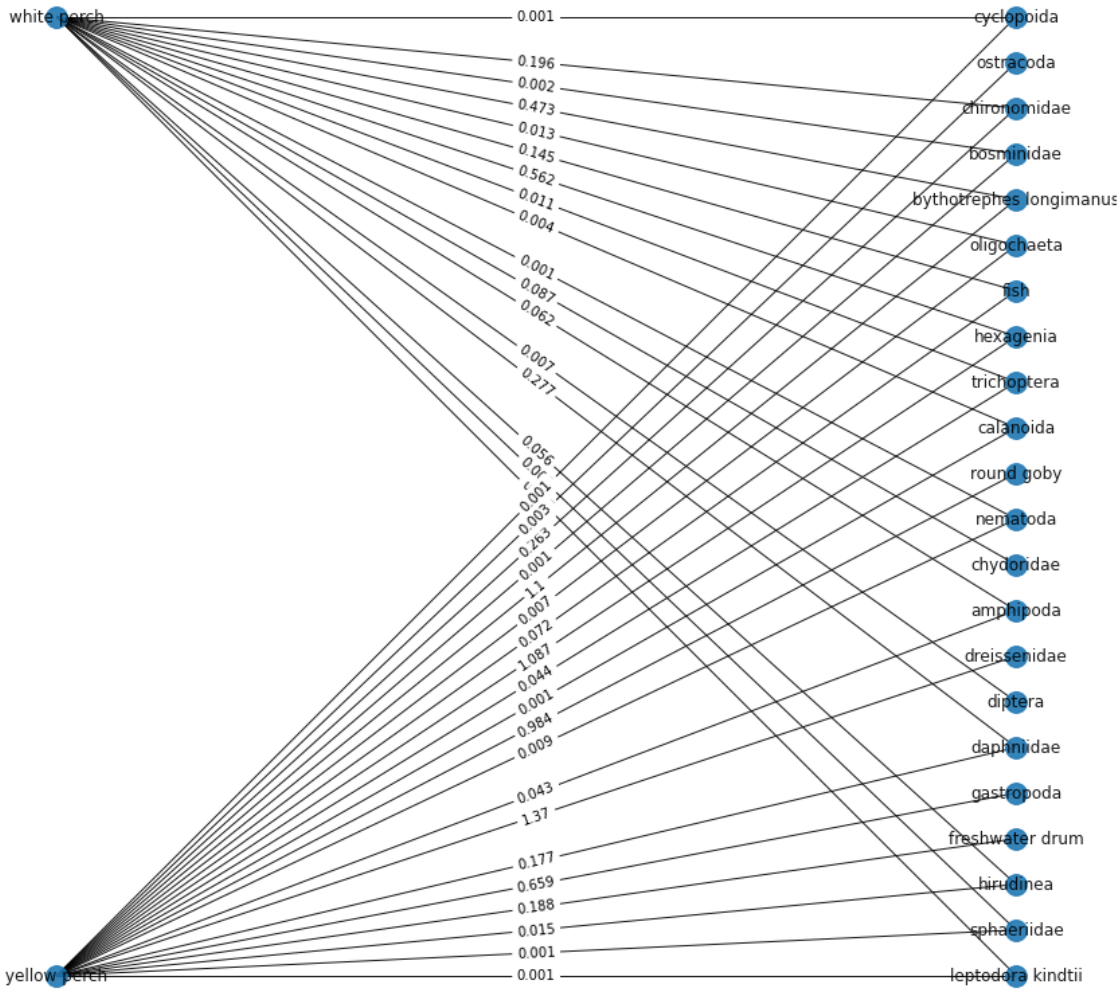

Figure 21: Both perch species consumed prey type and amount in grams for 2016

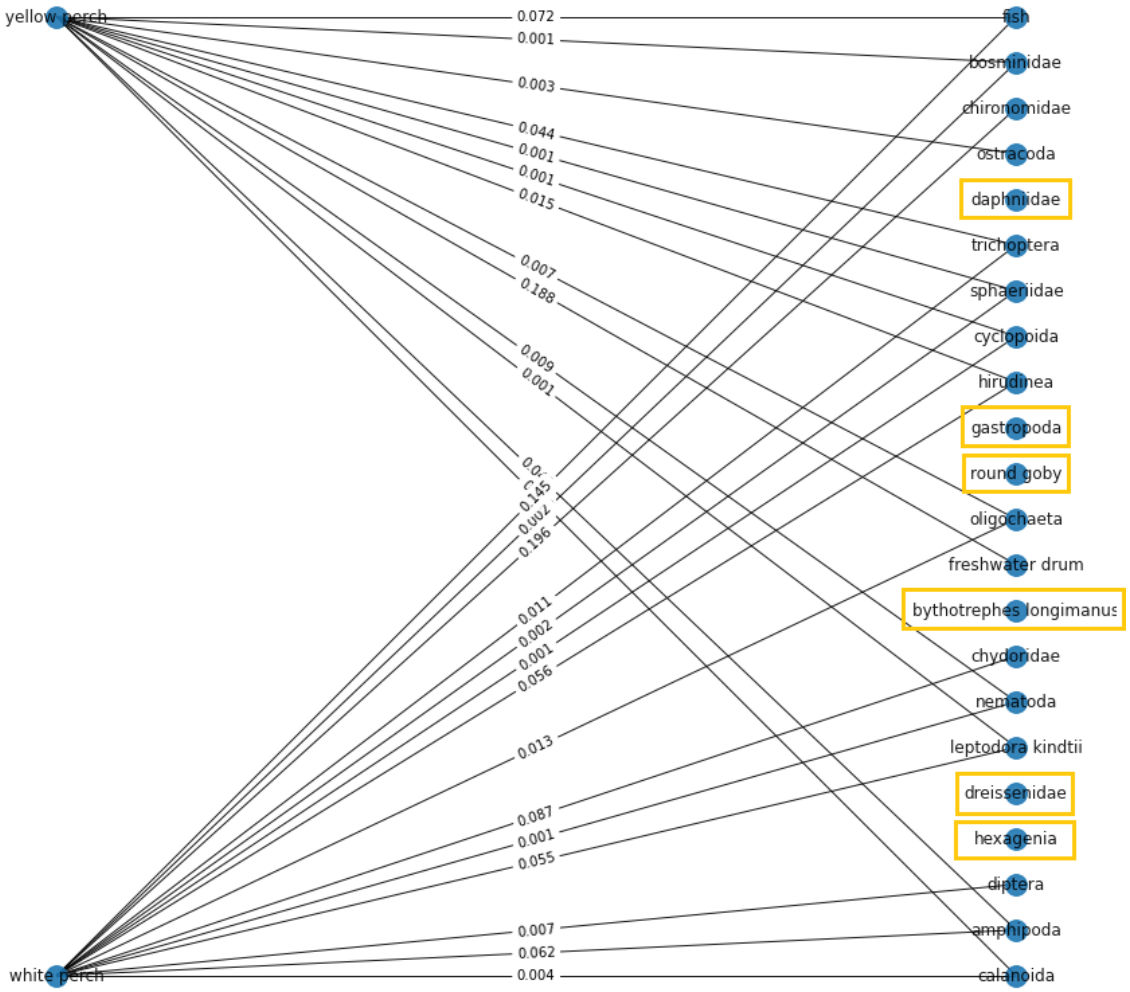

Figure 22: A disjoint set resulting from edge cuts made to Figure 21 when the prey weight was below 0.9 grams and consumed by both perch species in 2016. Prey no longer a member of the bipartite graph are boxed in yellow. This appears to be a notably competitive year since many remaining prey species are alike

Threshold Weight (g)	Year	Both perch species % of total prey weight lost
1.5	2014	19.3%
0.7	2015	8.5%
0.9	2016	12.9%

Figure 23: Percentage of prey weight in grams taken out from the total weight after edge cuts are made to Figures 17, 19, and 21

If we sum up the percentages in Figure 23, we observe 40.6% of the total weight is lost. That's nearly half the prey weight eaten for both species simultaneously! Thus, we further prove our point that making these edge cuts at the determined threshold weight will increase competition between species. It makes the perch go for the 'main' prey instead of the 'incidental' prey, which are consumed at lower weights and higher frequency according to Figure 1.

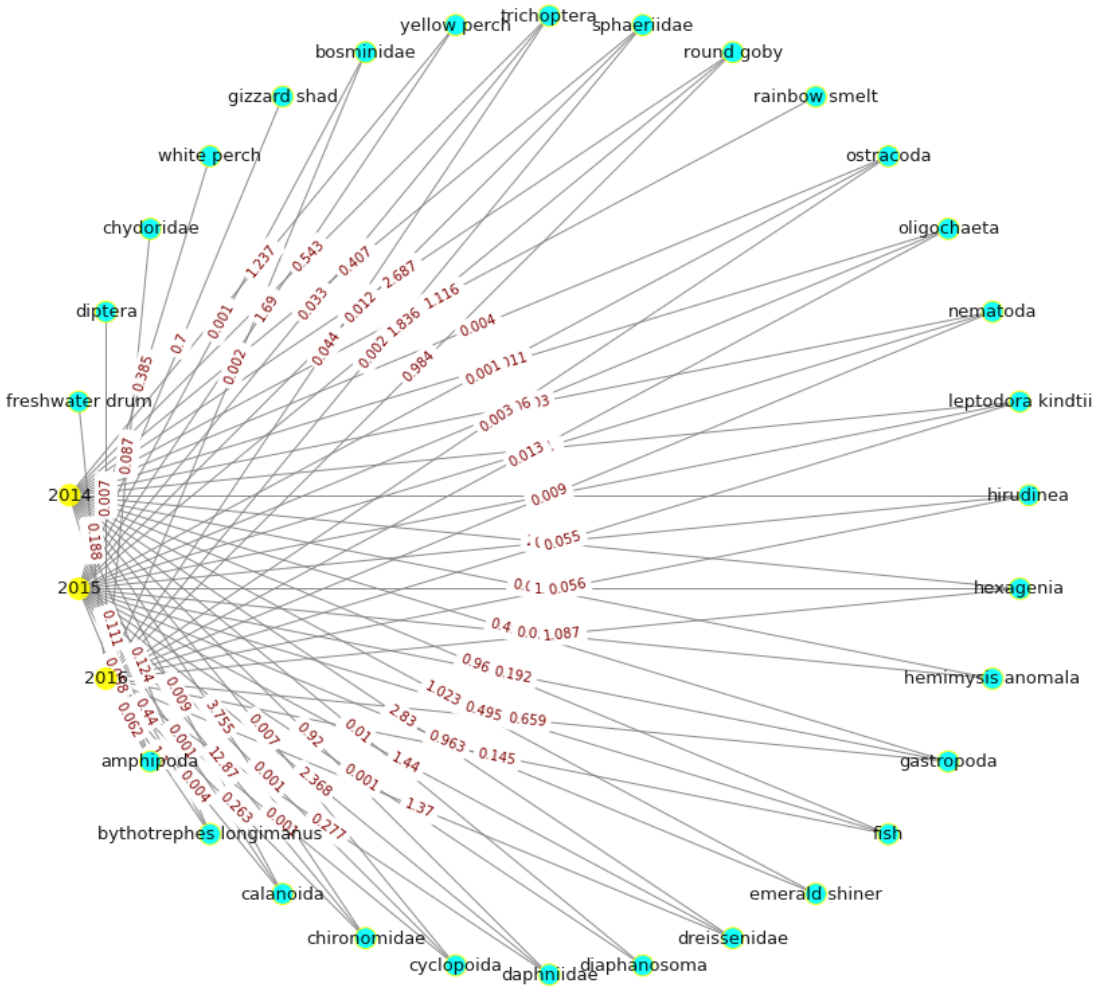

Figure 24: The amount of prey eaten in grams and which year(s) it was consumed

We move on to Figure 24 and see the following listed prey have a vertex degree of 3 by Definition 5. Those prey are trichoptera, sphaeriidae, round goby, ostracoda, oligochaeta, nematoda, leptodora kindtii, hirudinea, hexagenia, gastropoda, fish, dreissenidae, daphniidae, cyclopoida, chironomidae, bythotrephes longimanus, and amphipoda. Since these prey had a degree of 3, we know they were eaten every year. They account for 17 out of 29 nodes, or about 59% of the total number of prey nodes. Now we know just over half the prey in this data set are eaten all three years. We can also see that the most popular prey for white or yellow perch in Figure 16 (chironomidae, dreissenidae, round goby, and hexagenia) all have a degree of three in Figure 24. Thus, there must have been constant consumption and preferability of these prey, therefore supporting our earlier popularity attribution to them.

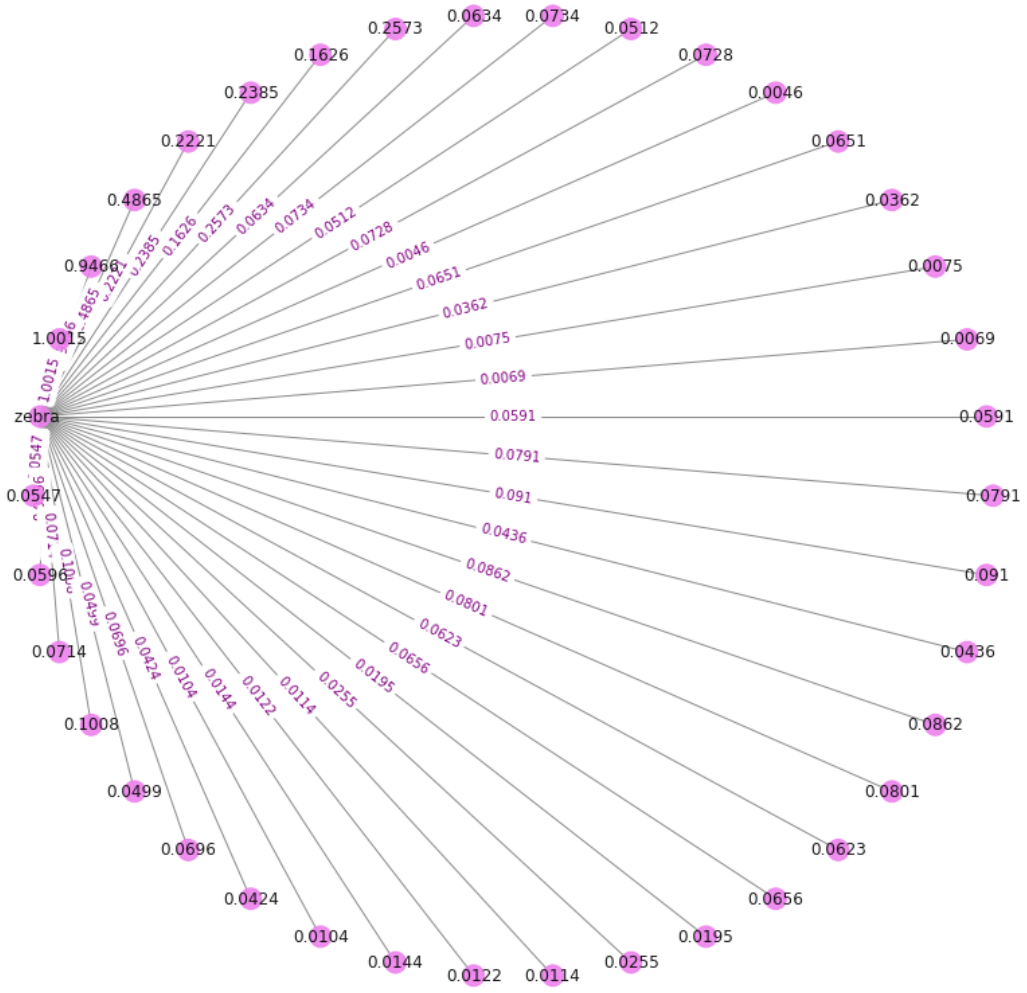

Figure 25: Zebra mussel dry weights for only flesh

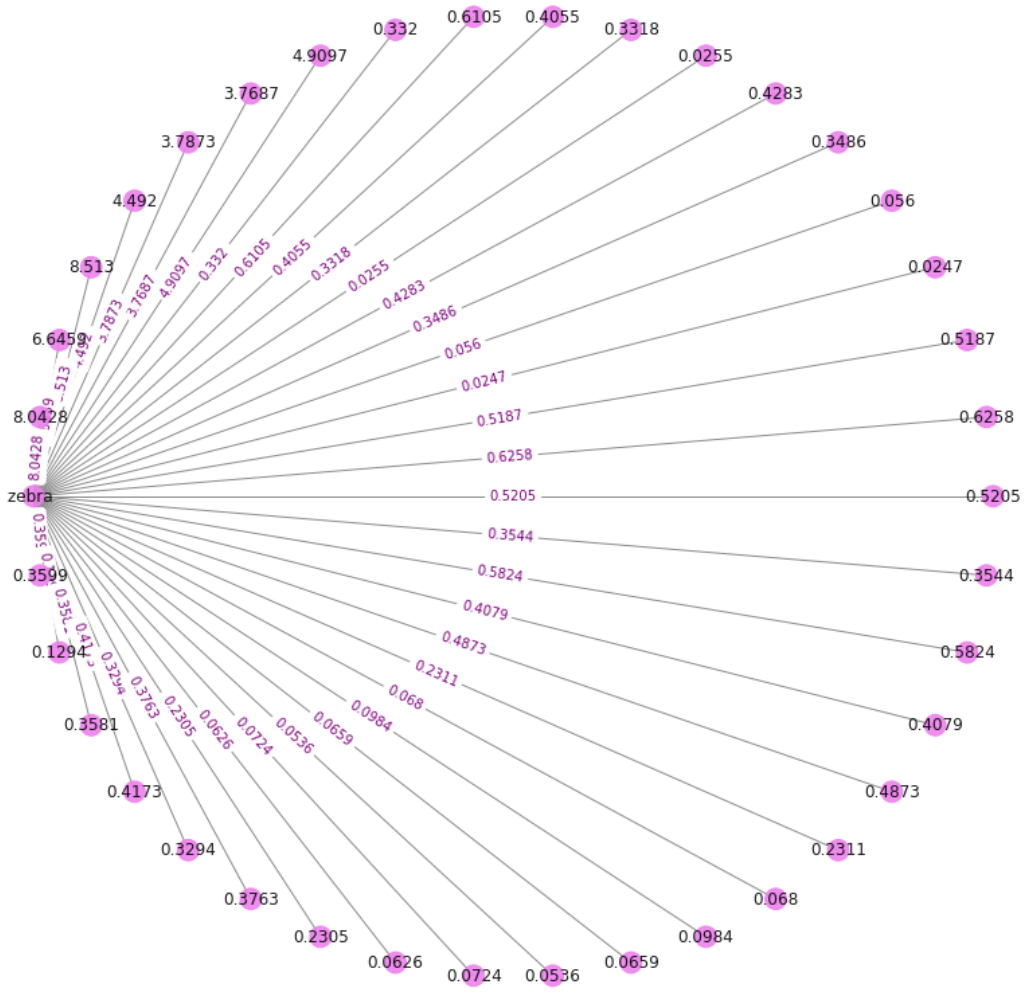

Figure 26: Zebra mussel dry weights for only shell

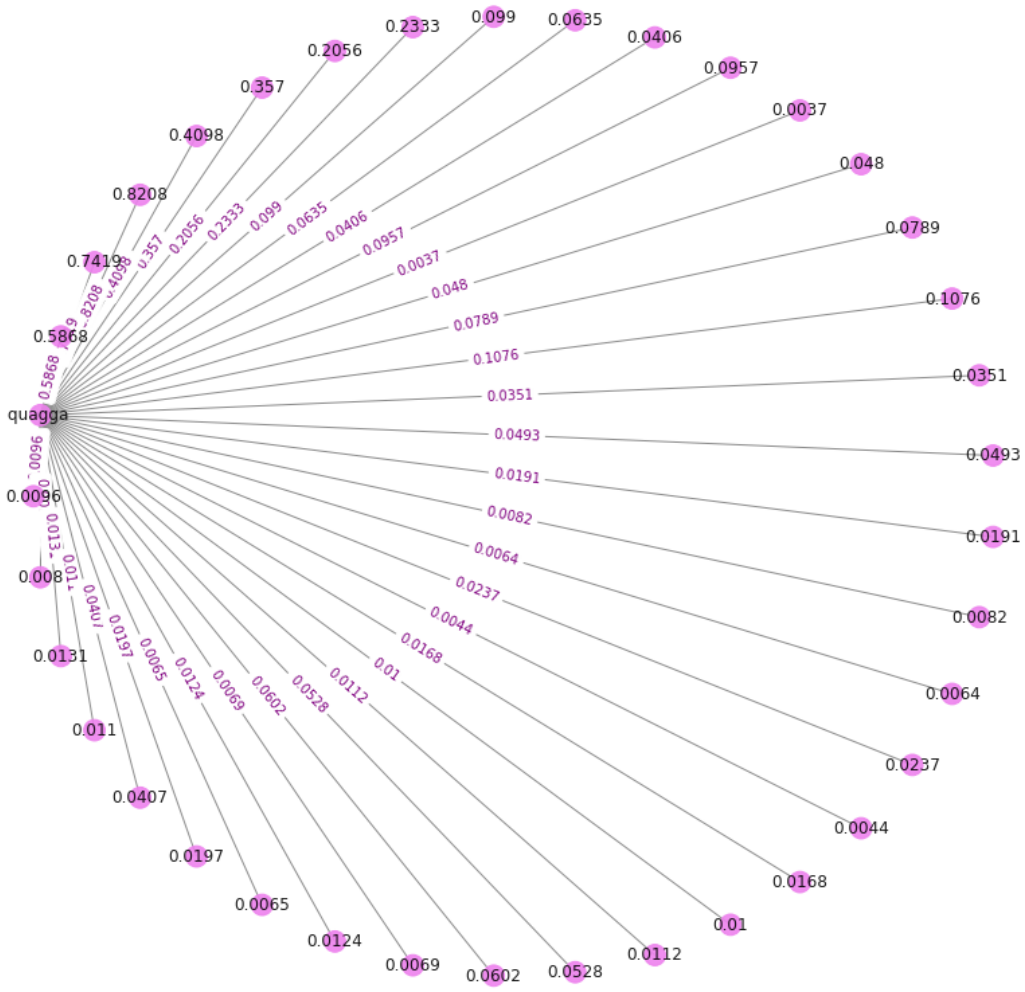

Figure 27: Quagga mussel dry weights for only flesh

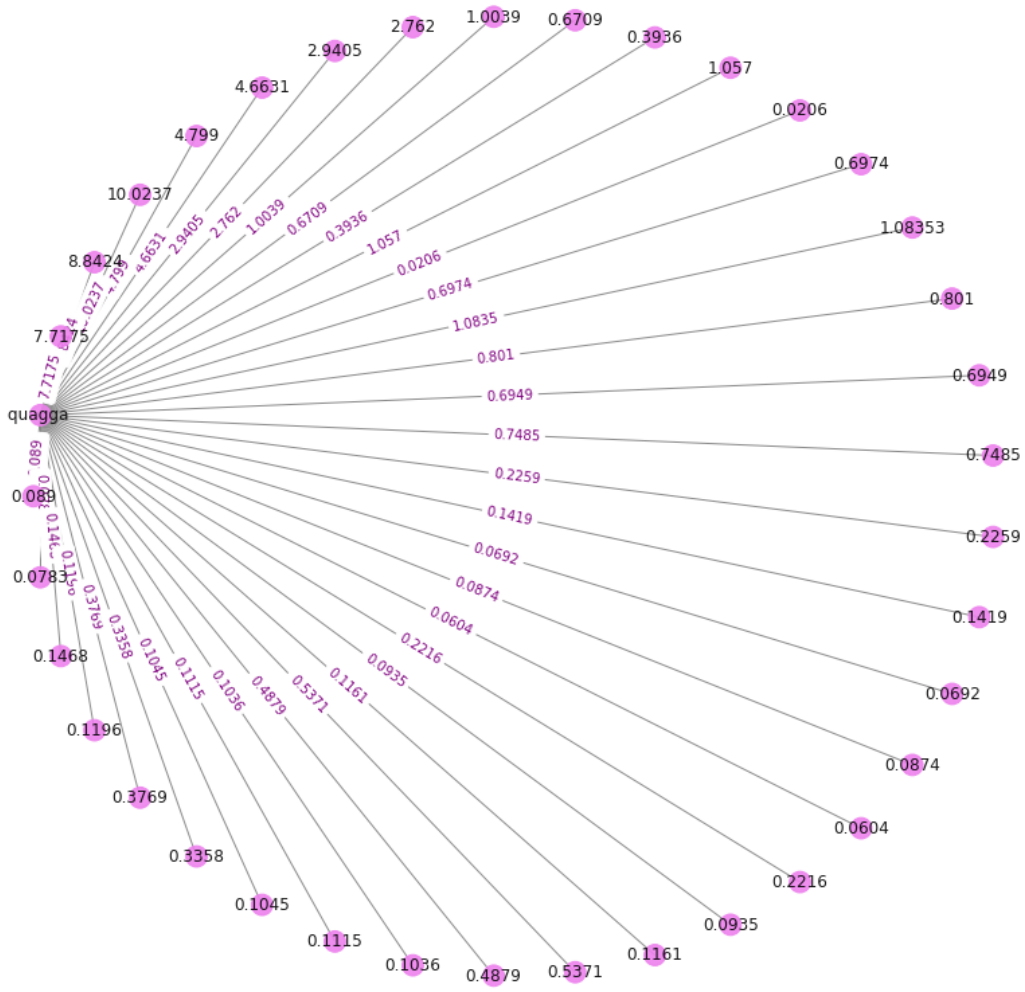

Figure 28: Quagga mussel dry weights for only shell

Zebra Mussel	Quagga Mussel
flesh: 4.8 grams	flesh: 4.3 grams
shell: 49.1 grams	shell: 52.5 grams

Figure 29: Dry weight sum by type of mussel specimen present

We find Figure 26 is higher at 49.1 g for our zebra mussel data by totaling the edge weights in Figures 25 and 26. With the same calculation for Figure 27 and Figure 28, we find Figure 28 is higher at 52.5 g for our quagga mussel data. This tells us invasive quagga mussels were eaten more, telling us either the fish preferred the invasive species or they were problematically more populous. These edge weight sums by mussel and dry weight type are depicted in Figure 29. A much larger weight of shell specimen was consumed by the sampled fish. Since both specimen types were taken from the fish, we know they have no preference between shell and flesh of the mussels. They eat the entire organism. Therefore, this large mussel consumption helps defend the popularity of dreissenidae in 2014 and 2016 for yellow perch (as seen in Figure 16).

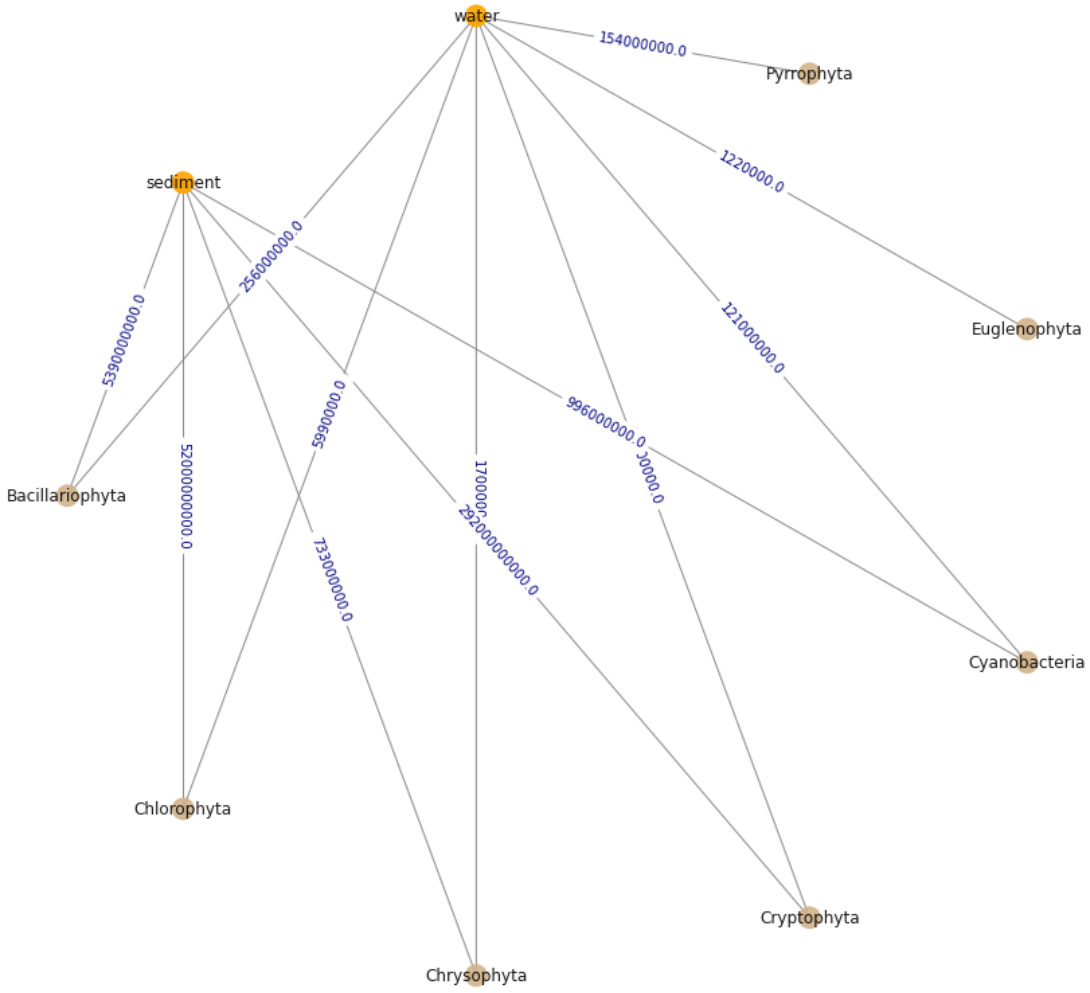

Figure 30: Biovolumes (cubic micrometers per liter) presented for divisions of phytoplankton specimens in sediment or water samples

Figure 30 details biovolumes in cubic micrometers per liter of phytoplankton specimens which were collected in either sediment or water samples. We inspect this graph to obtain a general view of ecosystem health. We sum phytoplankton biovolume by sample type. The sediment samples had a total of $6.27x10^{13}$ cubic micrometers per liter of phytoplankton. The water samples had a total of $5.68x10^{11}$ cubic micrometers per liter of phytoplankton.

Having Greek origins, "phyto (plant) and plankton (made to wander or drift), phytoplankton are microscopic organisms that live in watery environments, both salty and fresh" [7]. They can be protists, bacteria, sing-cell plants, and are more commonly known as "cyanobacteria, silica-encased diatoms, dinoflagellates, green algae, and chalk-coated coccolithophores" [7]. These types of phytoplankton are pictured in Figure 31.

Figure 31: Types and appearances of phytoplankton [7]

Photosynthesis provides chemical energy by chlorophyll capturing sunlight or in a few instances by also eating organisms [7]. Carbon dioxide, sunlight amount and strength, and nutrients such as nitrate, phosphate, silicate, or calcium all influence the growth and number of phytoplankton in an area of water [7]. If nitrates are low, they may be able to survive. Phytoplankton growth and abundance is also influenced by the temperature of the water, the salinity of the water, water depth, above surface winds, and predation [7]. Phytoplankton can rampantly grow as a bloom if the previously listed characteristics are met in decent or preferable amounts. Satellite images can visualize these blooms that can last many weeks. However, each phytoplankton lives for merely a couple of days.

A main base of the aquatic food web, they feed microscopic to large-scale organisms and can cause die-outs and diseases. A few species create "powerful biotoxins, making them responsible for so-called "red tides," or harmful algal blooms," and then those algal blooms kill aquatic species and even humans who consume the toxic food [7]. When a detrimental bloom occurs, dead phytoplankton sink to the ocean floor and are decomposed by bacteria, thus making a "dead zone" of life with depleted oxygen levels [7].

Phytoplankton are also a huge part of the carbon cycle. This is the circulation of carbon, which is a building block for life, through the lithosphere (solid Earth), hydrosphere (water), biosphere (life), and atmosphere (gasses). This cycle is pictured in Figure 32.

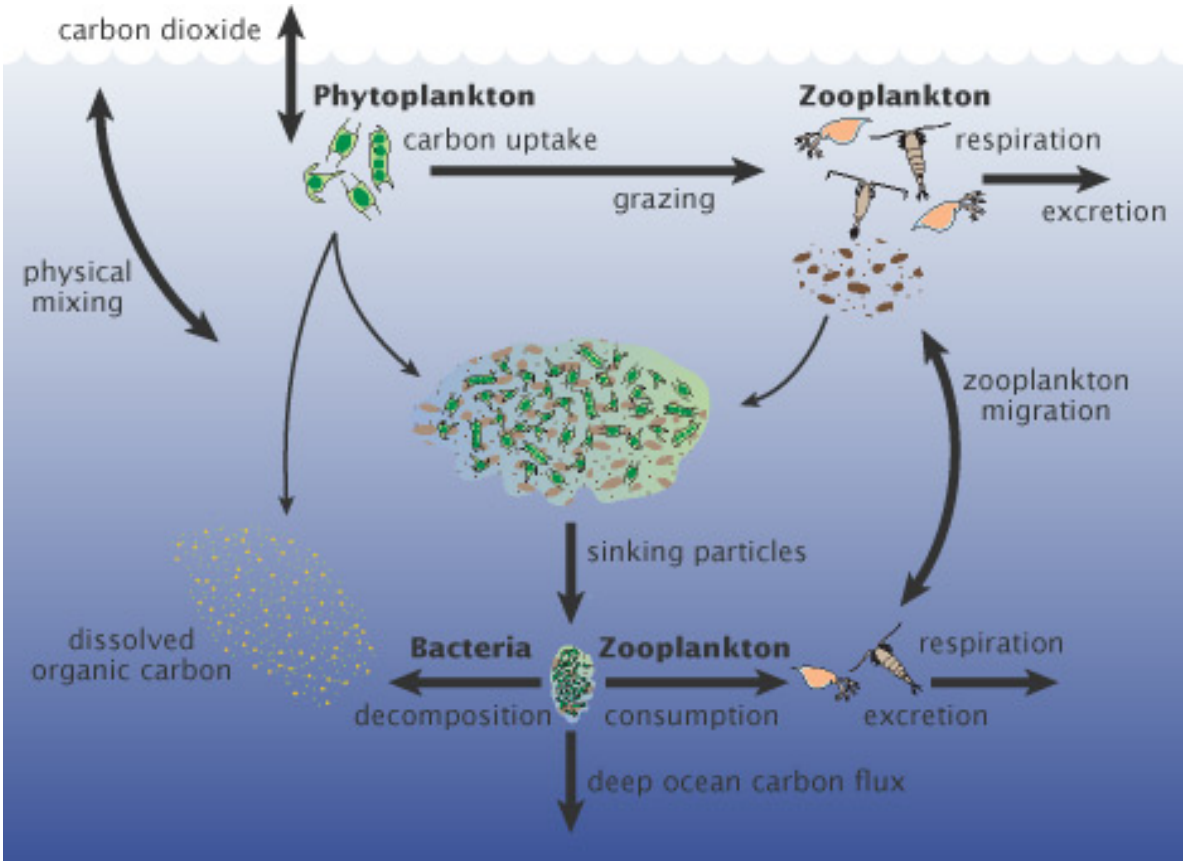

Figure 32: The role of phytoplankton in the carbon cycle. Through this process, ten gigatons of carbon travel from the atmosphere to the ocean each year [7]

As was done to collect the data we used from the USGS, samples can be obtained with hoses, flasks, or filters dragged behind a boat at observation stations [7]. To class samples by division in the dataset, scientists need genetic analytics or microscope technology. A bloom's high chlorophyll concentrations may add a green, red, or brown tint to the water. This is what helps determine biovolume, an aspect contained in our generated Figure 30.

Phytoplankton thrive near coastlines, continental shelves, and the equator [7]. Winds affect water currents, and thus move the organisms across water bodies. This causes the uplifting of nutrients from the depths. Due to this process, phytoplankton can directly affect ecosystem health. As water temperatures increase, greenhouse gasses become more prevalent. Thus, phytoplankton productivity will decrease with "less vertical mixing to recycle nutrients from deep waters back to the surface" [7]. Figure 33 indicates where phytoplankton exist in high amounts due to higher chlorophyll contents. Figure 34 indicates where phytoplankton numbers decrease due to chlorophyll content lowering from rising ocean temperatures [7]. Therefore depicting a clear cause and effect relationship.

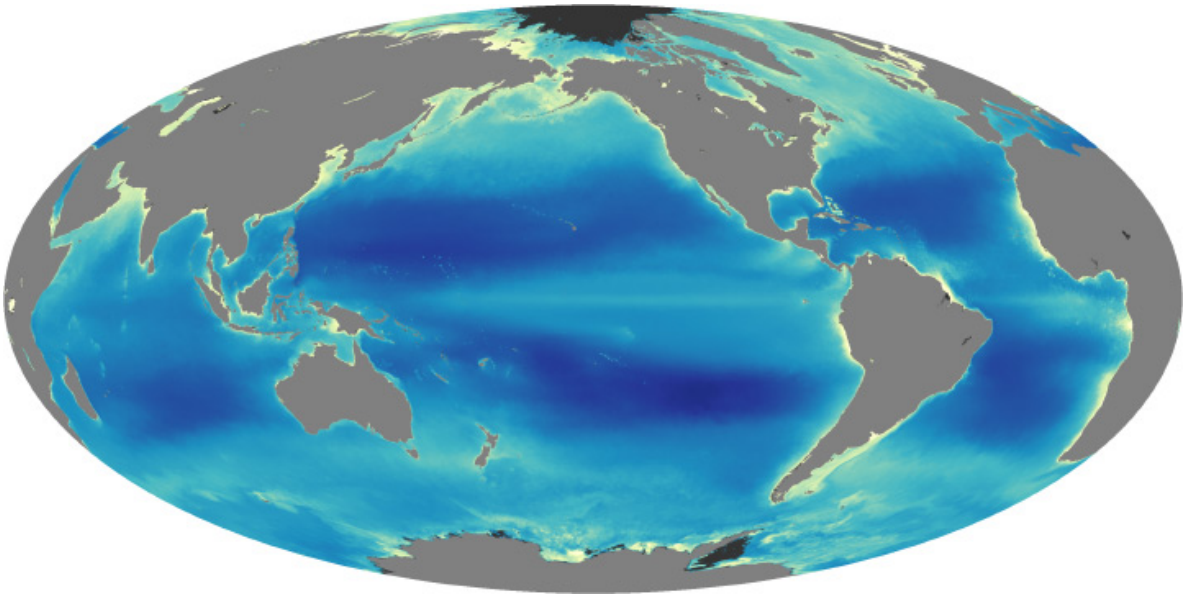

Figure 33: Yellow indicates high chlorophyll content where phytoplankton are very abundant and dark blue indicates areas where they are less abundant due to low nutrient contents. These traits are indicated from July 2002 to May 2010 [7]

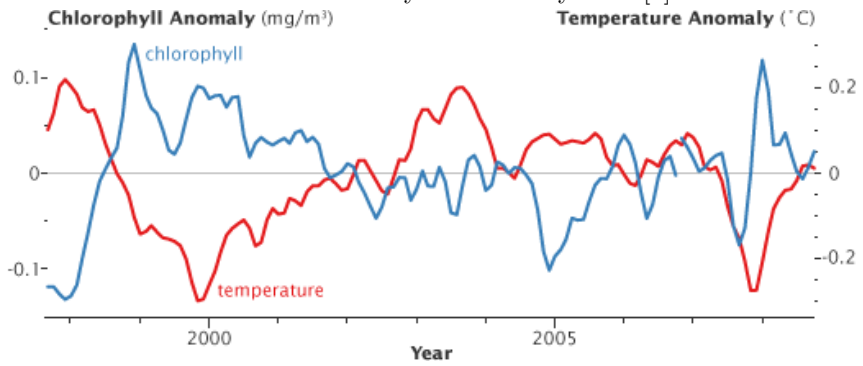

Figure 34: Chlorophyll content (blue line) decreases when high-than-normal average temperatures increase (red line) [7]

From all this information, we conclude that having a higher amount of phytoplankton in the sediment samples as compared to the water samples results in a likely healthier western basin of Lake Erie. If there were an excess of phytoplankton in the water, harmful algal blooms with subsequent de-oxidation and the deaths of marine life would likely occur. This also means that nutrients are being upturned, carbon is being cycled, and water temperatures are staying at a healthy level. Thus, we have obtained a general viewpoint of ecosystem health in this locality of Lake Erie.

4 Conclusion and Directions for Further Research

Our main focus of this research has been the use of site-collected samples and data. Another possible approach could be the use of satellite data. Satellites can supply global-scale information and analysis. We know phytoplankton by themselves are small, but together they can bloom billions at a time and change how the surface reflects light with varying chlorophyll concentrations [7]. This tinting effect can be seen in Figure 35. Colors in the ocean surface that Figure 35 depicts are the sensors collecting and characteristically grouping the colors into categories for computer aided analysis. Yet, this method of data collection is difficult as satellite imagery available to the public is a relatively recent resource and can be difficult for future predictions. Satellite data can also be limited when the study becomes increasingly specific. For this reason, we suggest further research with satellite imagery should utilize data involving aspects that directly affect Lake Erie as a larger ecosystem. Then take that aspect

analysis from a top-down approach for a more specific perspective of the ecosystem. If seeking to know about Lake Erie's phytoplankton inhabitants, we advise using frequently reported satellite water temperature data. An aspect that affects phytoplankton growth rates at a microscopic level.

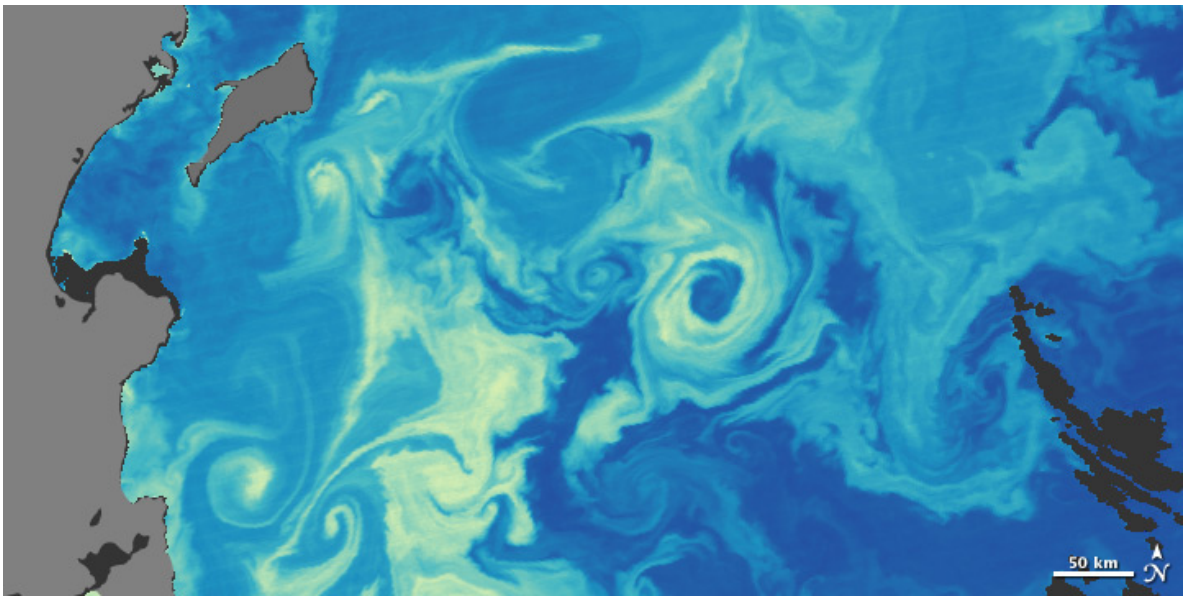

Figure 35: A natural-color satellite image of chlorophyll concentration near Kamchatka, Russia on June 2, 2010. Yellow indicates a high chlorophyll concentration and thus high concentrations of phytoplankton [7]

Figure 35 is an example of the use of satellite imagery to study global phytoplankton productivity. Oceanographers have seen an increase of phytoplankton in subtropical ocean gyres over the past 10 years where the area has typically been less productive [7]. "These low-nutrient 'marine deserts' appear to be expanding due to rising ocean surface temperatures," and are thus a direct indicator of climate variability [7]. This shows how satellite imagery can be used for future climate investigations on a global-scale as opposed to the top-down approach suggested above.

Feature layers are groupings of similar geometric properties as points, lines, or polygons which can be displayed on a map in ArcGIS Pro to visualize data. Put more simply, feature layers represent objects like rivers or fishing spots as vectors. Questions can be raised as to why a year gap in dreissenidae's high popularity occurred between 2014 and 2016 in Figure 16. We can better understand this gap by utilizing the software ArcGIS Pro or its web version and see if mussel data is available as feature layers or other mappable data types. Additional data can be found from the USGS or any other certified reporting agency to better understand why this gap occurred. With this information, we still leave the kinds of found or created data for further research up to the reader.

In this study, we have discerned the most popular prey type by year. By making edge cuts at or below a threshold value, we have determined the amount of total prey weight or consumed prey lost. This has directly influenced the existence or increase of competition between the two species. We have also determined this information for both perch species simultaneously in larger bipartite graphs. Forming another perspective on the same data, we have discerned that prey were popular simply because they were consumed all three years by node degree. After that we have helped prove an earlier yellow perch prey popularity conclusion while looking at one prey type's dry weight consumed. Lastly, we looked at which type of sample contained more phytoplankton. Learning about what phytoplankton are and their effects on the environment have given a broader understanding. We have learned how their abundance correlates with variations in water temperature, chlorophyll content, algae bloom growth, nutrient cycling, and the ever important carbon cycle.

Overall, this analysis has provided a concrete understanding of possible or existing diet, competition, and popularity trends for white and yellow perch in the western basin of Lake Erie during a 2014 to 2016 time frame.

References

[1] Kevin R Keretz. Richard T Kraus. Joseph D Schmitt. Lake Erie Fish Community Data, 2013-2021. https://www.sciencebase.gov/catalog/item/61e87616d34e8b818ad89732, 2022.

[2] Kevin R Keretz. Richard T Kraus. Joseph D Schmitt. Zebra and Quagga Mussel Dry Weight Information; Lake Erie 2014. https://www.sciencebase.gov/catalog/item/5e4e9afae4b0ff554f70cb37, 2020.

[3] Mary A Evans. Emily E Wimmer. Phytoplankton Community Composition in Western Lake Erie, 2014-2018; Grand Traverse Bay, Lake Michigan, 2015; and Saginaw Bay, Lake Huron, 2015. https://www.sciencebase.gov/catalog/item/604fbd36d34eb1203122c015, 2021.

[4] Maarten van Steen. Graph Theory and Complex Networks: An Introduction. http://www.math.wm.edu/~rrkinc/homework/GTCNslides2.pdf, 2014.

[5] Daniel Freeman. Discrete Math: Lecture 15. https://mathstat.slu.edu/~freeman/Discrete_Lecture_15.pdf, n.d.

[6] Marc Los Huertos. Dreissenidae: The Players: Evolving Aquatic Species. https://www.sciencedirect.com/topics/agricultural-and-biological-sciences/dreissenidae, 2020.

[7] Rebecca Lindsey. Michon Scott. What are Phytoplankton? https://earthobservatory.nasa.gov/features/Phytoplankton#:~:text=Phytoplankton%20cause%20mass%20mortality%20in%20other%20ways.%20In,animal%20life%3B%20the%20result%20is%20a%20dead%20zone, 2010.

5 Appendix

https://www.dropbox.com/sh/olaz92nemjmywd3/AACKVy0ET1BydHUCfuqX84f-a?dl=0

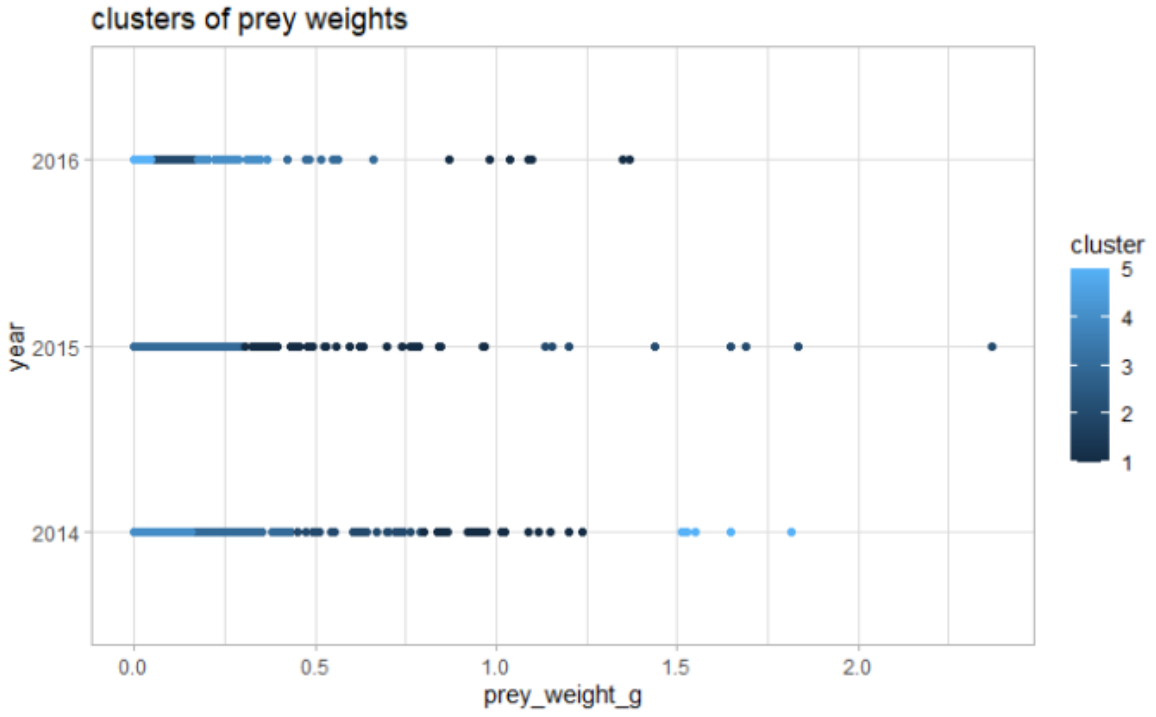

Figure 1: This cluster graph reiterates our threshold points by displaying breaks in clustering where our prey weight grams of 1.5, 0.7, and 0.9 lie on the x-axis